From Fossil Energy to Clean Hydrogen: Towards a Decarbonized Economy

UCI Combustion Institute – Summer School 2023
August 20 – 25, 2023

Reginald E. Mitchell

Professor of Mechanical Engineering, Emeritus
Stanford University
and
Senior Advisor, Office of Fossil Energy and Carbon Management
Division of Hydrogen with Carbon Management,
U.S. Department of Energy

From Fossil Energy to Clean Hydrogen: Towards a Decarbonized Economy

Abstract

Greenhouse gas (GHG) emissions are causing the temperature of the Earth's surface to increase and in order to limit this temperature rise, our emissions of greenhouse gases must approach net-zero levels in the near future. Recent legislature supported by President Biden has set the U.S. on a course to reach net zero GHG emissions economy-wide by no later than 2050, limiting the temperature rise to 1.5 degrees Celsius. To meet this goal, the U.S. is transitioning to a net-zero GHG emissions economy, shifting from using fossil energy-based fuels to using carbon-free fuels, in particular, hydrogen. This transition will be across nearly all sectors of the economy, including, the aviation, chemicals, cement, iron & steel, maritime, oil & gas, power, and transport sectors.

Since molecular hydrogen does not exist in appreciable quantities on Earth, if hydrogen is to become the fuel of the 21st century, methods of producing it from coal, biomass, natural gas, plastics, municipal solid waste, and other wastes must become more efficient and cost-effective. In this presentation, electrolysis, gasification, reforming, and pyrolysis are briefly discussed as clean hydrogen production technologies when coupled with technologies for carbon capture and storage. When renewable fuels are used as feedstocks, these technologies are capable of net-zero GHG emissions.

Before talking about these hydrogen production methods, I will discuss a study that involved characterization of the chemical reactivities of coal and biomass chars. Being able to predict the consumption rates of chars permits the optimization of gasifiers for hydrogen production. I will next discuss a study focused on developing carbon-based fuel cells that can be used to produce hydrogen from coal and biomass. I will end the talk with a discussion of present-day, hydrogen production technologies.

From Fossil Energy to Clean Hydrogen: Towards a Decarbonized Economy

Lecture Outline

- Educational and Professional Background
- Carbon Conversion Investigations
  - Coal and biomass char combustion & gasification kinetics studies
  - Carbon-based solid oxide fuel cell studies
- Hydrogen - The Fuel for the 21st Century
  - Hydrogen production
- Questions

Education

Jack Yates Senior High School (in 1958)
Houston, Texas

UNIVERSITY of DENVER

Bachelor of Science Degree in
Chemical Engineering (BSChE)

NJIT New Jersey Institute of Technology

Master of Science Degree in
Chemical Engineering (MSChE)

Thesis: Feedforward, Feedback Control of a Fluidized Bed Reactor

MIT Massachusetts Institute of Technology

Doctorate of Science (ScD)
in Chemical Engineering

Thesis: Nitrogen Oxide Formation in Laminar Methane-Air Diffusion Flames

Professional Experience

Sandia National Laboratories

- Member of the Technical Staff
- Distinguished Member of the Technical Staff

Research Activities

- Acetylene Oxidation/Pyrolysis
  Reaction mechanisms
  Reaction kinetics
- Coal char oxidation
  Mass loss and temperature measurements
  Reaction mechanism and kinetics

Stanford University

- Associate Professor
- Professor

Teaching

- Thermodynamics
- Radiation Heat Transfer
- Combustion Fundamentals
- Combustion Applications
- The Science of Flames

Research Activities

- Coal/biomass char particle oxidation studies
- Coal/biomass char particle gasification studies
- Copper particle oxidation
- Supercritical water oxidation
- Carbon-fueled solid oxide fuel cells

- Senior Advisor
  Office of Fossil Energy and Carbon Management
  Division of Hydrogen with Carbon Management

Kinetic studies of the intrinsic reactivities of char particles in environments containing specified concentrations of O_2, CO_2 and H_2O at specified temperatures

Ph.D. Students: Nancy Tsai, Paul Campbell, Bum Jick Kim, Matthew Tilghman

Research Approach: Char Combustion Studies

Overall Objective: To develop the capability to predict the chemical reactivities of coal and biomass chars in environments characteristic of combustors and gasifiers.

- A laminar flow reactor was designed that permitted coal and biomass particles to undergo devolatilization and char burnout in environments similar to the environments established in real combustors and gasifiers.
- Char particles were extracted from the flow reactor just subsequent to devolatilization. Char mass loss rates under chemical kinetic-controlled conversion conditions were measured in experiments performed in a pressurized thermogravimetric analyzer (PTGA).
- The intrinsic chemical reactivities of the chars were determined from measured mass loss and specific surface area data and a heterogeneous chemical reaction mechanism was developed that described the intrinsic reactivities.

  Data were used to adjust kinetic parameters in a reaction mechanism that describes key reaction pathways when carbon reacts with oxygen, carbon dioxide, and water, in the presence of carbon monoxide and hydrogen.

Laminar Flow Reactor

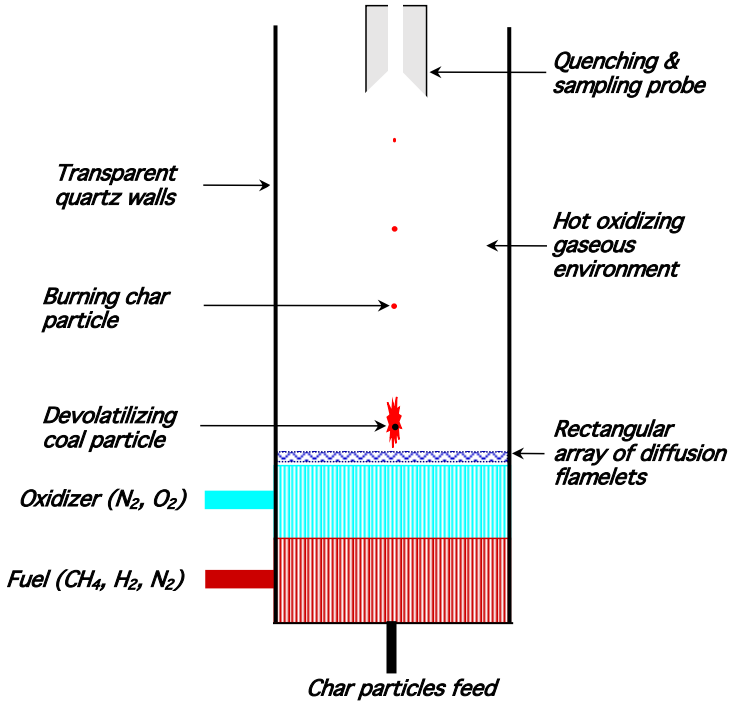

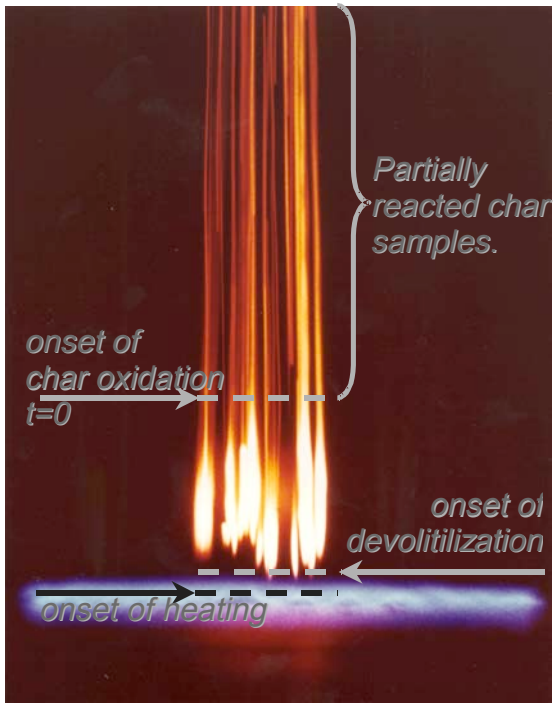

Pressure: 1 atm
Temperature: 1250 – 2100 K
[O_2]: 0 – 21%

Coal Char Particles

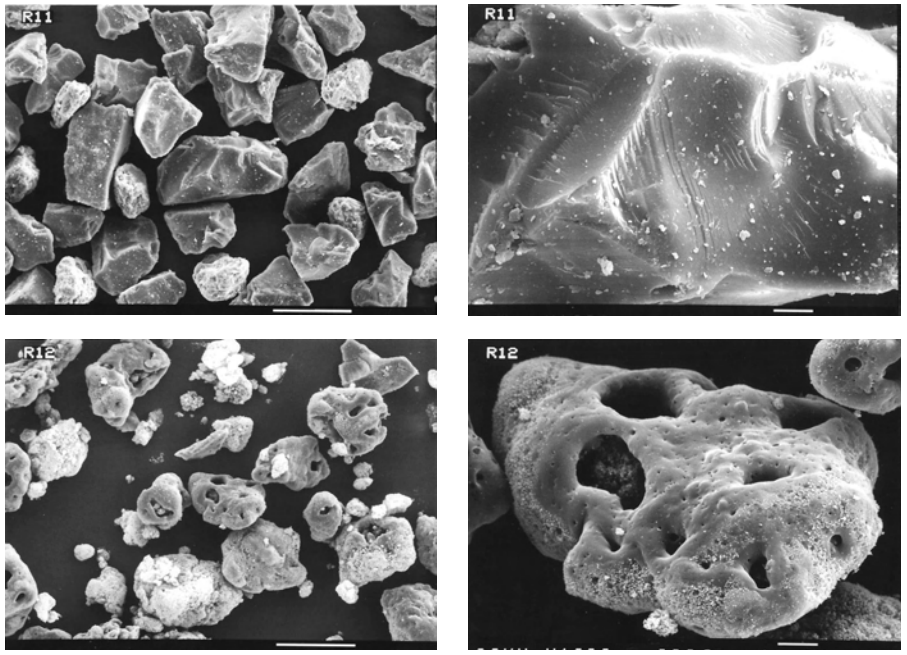

Raw Coal:
t = 0 ms
0% conversion

Coal Char:
t = 47 ms
54% conversion

Scanning electron micrographs of bituminous coal particles.
Raw coal particles were normally 100 μm in size.

Thermogravimetric Analyzer

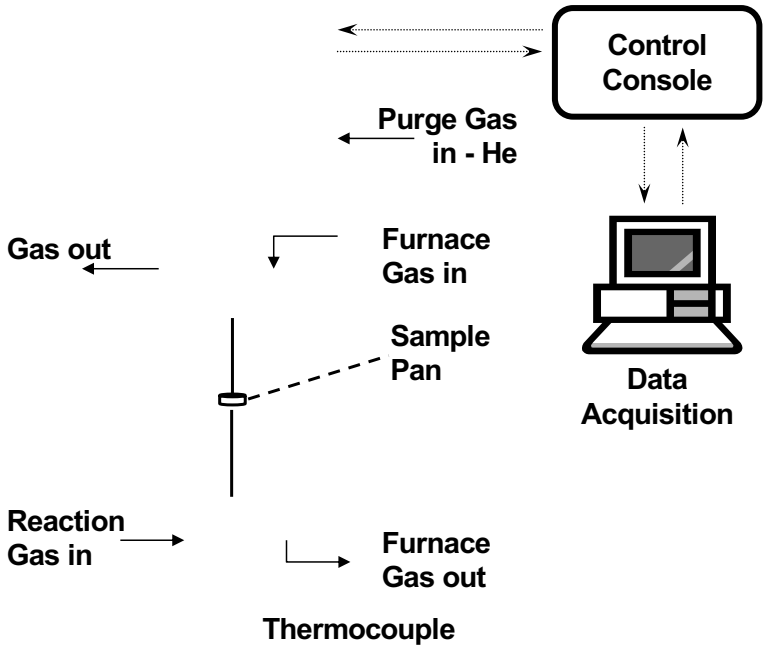

Composition: inert and oxidizing
Pressure = 10^{-5} torr – 100 atm
Temperature = 298 to 1373 K
Weight Range = 0 – 10 g Accuracy = 10^{-6} g

Char Mass Loss Rates

Char normalized mass loss rates are calculated from the measured PTGA thermograms, obtained over a range of temperatures, pressures and compositions that render kinetics-limited conversion rates.

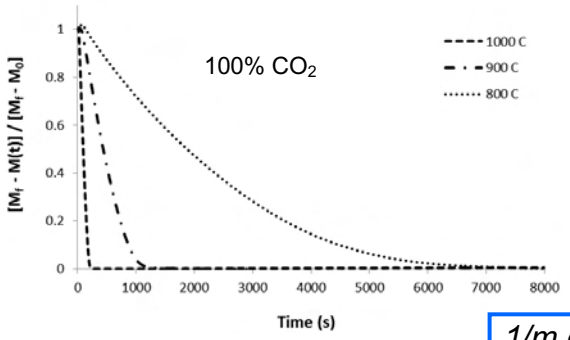

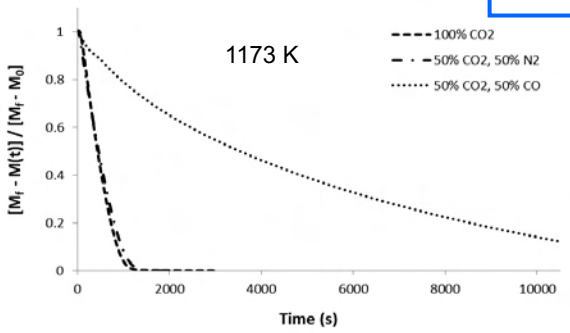

1/m dm/dt = f(x)

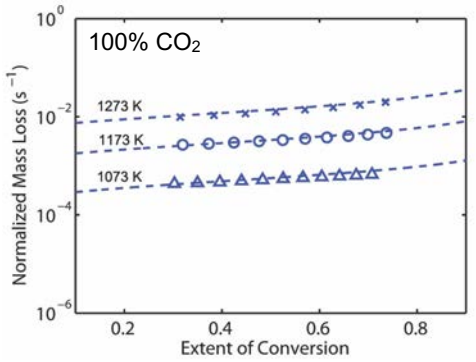

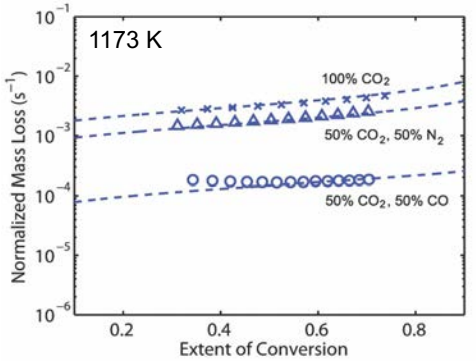

Intrinsic Char Reactivity

Char reactivity is calculated from the measured PTGA thermograms, obtained over a range of temperatures, pressures and compositions that render kinetics-limited mass loss rates.

Rate of Char Conversion

$$-\frac{1}{m_C}\frac{dm_C}{dt} = \frac{1}{1-x_C}\frac{dx_C}{dt} = R_{i,C}S_{gc}$$

$R_{i,c}$ ==> intrinsic char reactivity [g/m^2/s]
S_{gc} ==> specific surface area of char [m^2/g]
m_c ==> mass of char [g]
x_c ==> conversion
t ==> time [s]

Both S_{gc} and $R_{i,c}$ vary with conversion and/or time.

Specific Surface Area Evolution

BET specific surface area was measured during the course of conversion in selected gasification tests. The structural parameter Ψ in the specific surface area model was adjusted to provide agreement with measurements.

$$S_g = S_{g,0}\sqrt{1-\psi\ln(1-x_c)}$$

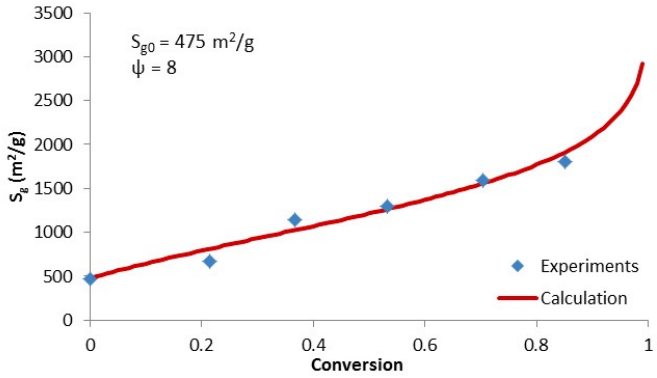

Char Specific Surface Area

BET specific surface areas of chars are measured in the PTGA using CO_2 as the adsorption gas at 10 atm.

CO_2 adsorption test performed on a char sample in the PTGA sample pan. (top) Observed weight is due to adsorbed CO_2 plus buoyancy and drag effects. (bottom) Empty pan runs. Observed weight is due to buoyancy and drag effects on pan.

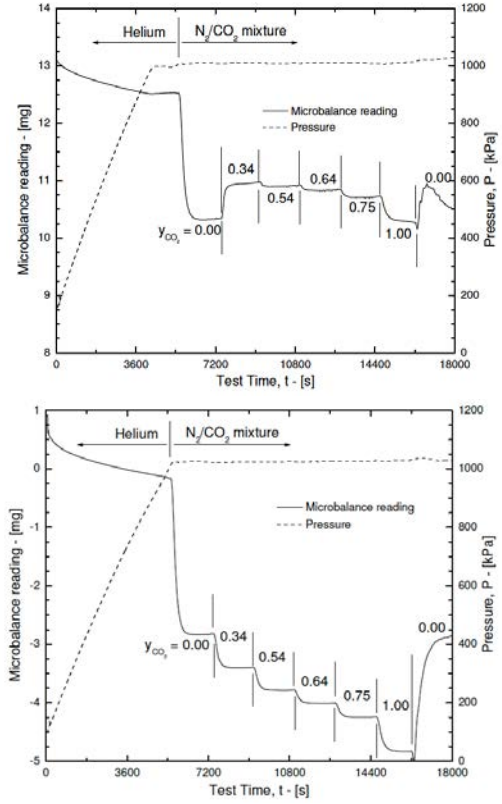

BET plot

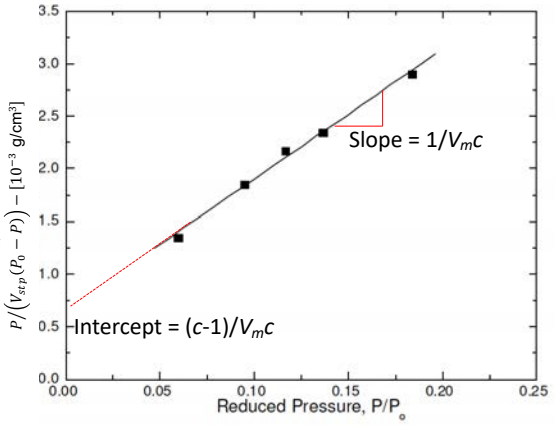

$$V_{stp} = \frac{m_{CO_2} \Re T_{stp}}{\tilde{M}_{CO_2} P_{stp}}$$

P_0 = saturation pressure

$$S_g = \frac{V_m A_m N_{AV} P_{stp}}{\Re T_{stp}}$$

For CO_2, A_m = 22.2 Å^2

Oxy-Reactivity Tests

Conditions of TGA oxi-reactivity tests

Test No.	Sample Name‡*	Test A or B	T_{rxn} – K	$[O_2]$ – mol-%	P_{rxn} - atm
1	SynChar‡-000*	A	673	6	1
2	SynChar-000	A	723	6	1
3	SynChar-000	A	773	6	1
4	SynChar-000	A	823	6	1
5	SynChar-000	A	873	6	1
6	SynChar-000	A	773	2	3
7	SynChar-000	A	773	2	5
8	SynChar-000	A	773	10, 6, 10, 2	1
9	SynChar-072	A	773	6	1
10	SynChar-117	A	723	6	1
11	SynChar-117	A	773	6	1
12	SynChar-117	A	823	6	1
13	LowKitt-072	A	773	6	1
14	LowKitt-117	A	723	6	1
15	LowKitt-117	A	773	6	1
16	LowKitt-117	A	823	6	1
17	CarbSph-000	A	723	6	1
18	CarbSph-000	A	773	6	1
19	CarbSph-000	A	823	6	1
20	SynChar-000	B	773	6	1
21	SynChar-117	B	773	6	1
22	LowKitt-117	B	773	6	1
23	CarbSph-000	B	773	6	1
24	WdChip-000	B	773	6	1
25	GlosPap-000	B	773	6	1
26	NewsPap-000	B	773	6	1

‡ SynChar = Synthetic Chars. LowKitt = Lower Kittanning Coal. CarbSph = CarboSphere®.
WdChip = Wood Chars. GlosPap = Glossy Paper Chars.
* Numerical characters correspond to residence time in the LFR (in ms).

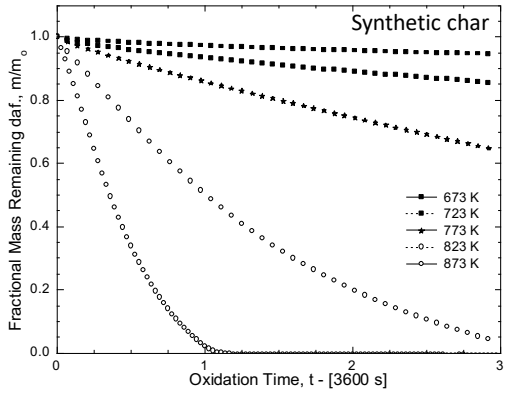

P_{O2} = 0.06 atm, P_{total} = 1 atm

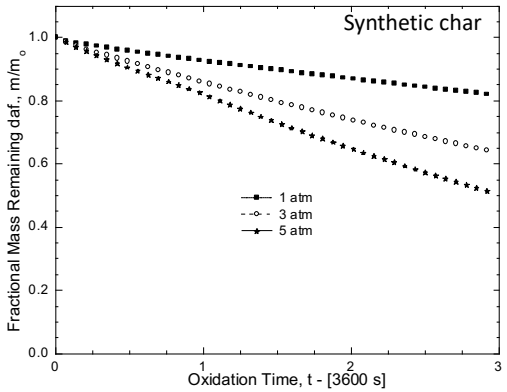

x_{O2} = 0.06, T = 773 K

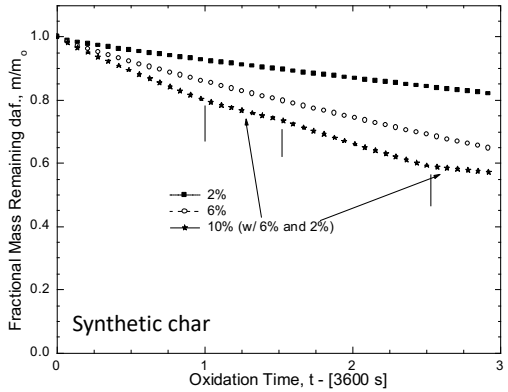

P_{total} = 1 atm, T = 773 K

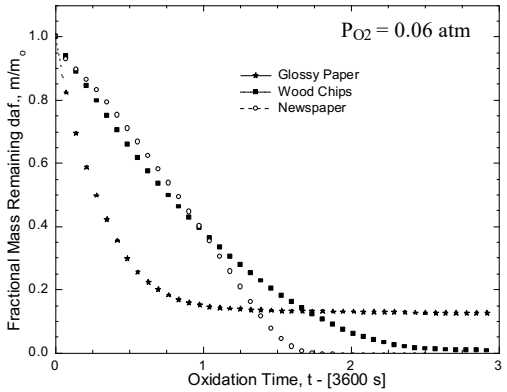

P_{total} = 1 atm, T = 773 K

Detailed Carbon Oxidation Mechanism

$$-C + O_2 \underset{phy,b}{\overset{phy,f}{\rightleftharpoons}} -C\text{-}(O_2)$$

Physisorption

$$-C\text{-}(O_2) + -C \xrightarrow{chm0} -C(O^m) + -C(O^m)$$
$$-C\text{-}(O_2) + -C + -C\text{-} \xrightarrow{chm1} CO + -C(O^m) + -C$$
$$-C\text{-}(O_2) + -C + -C\text{-} \xrightarrow{chm2} CO_2 + -C + -C$$

Chemisorption

$$-C\text{-}(O_2) + -C(O) + -C\text{-} \xrightarrow{chm3a} CO + -C(O^m) + -C(O^m)$$
$$-C\text{-}(O_2) + -C_2(O_2) + -C\text{-} \xrightarrow{chm3b} CO + -C(O^m) + -C(O^m) + -C(O^m)$$
$$-C\text{-}(O_2) + -C(O) + -C\text{-} \xrightarrow{chm4a} CO_2 + -C(O^m) + -C$$
$$-C\text{-}(O_2) + -C_2(O_2) + -C\text{-} \xrightarrow{chm4b} CO_2 + -C(O^m) + -C(O^m) + -C$$

Complex enhanced chemisorption

$$-C(O^m) \xrightarrow{mig1} -C(O)$$
$$-C(O^m) + -C(O) \xrightarrow{mig2a} -C_2(O_2)$$
$$-C(O^m) + -C_2(O_2) \xrightarrow{mig2b} -C_2(O_2) + -C(O)$$
$$-C(O) \xrightarrow{mig3a} -C(O^m)$$
$$-C_2(O_2) \xrightarrow{mig3b} -C(O^m) + -C(O)$$

Surface migration

$$-C(O) + -C\text{-} \xrightarrow{des1} CO + -C$$
$$-C_2(O_2) + -C\text{-} \xrightarrow{des2} CO_2 + -C + -C$$

Desorption

The complex -C(O) is representative of carbonyl and ether -type complexes, while $-C_2(O_2)$ is representative of lactone and acid anhydride -type complexes.

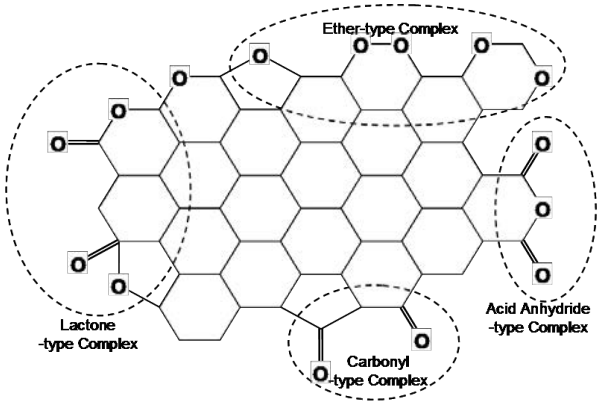

Distribution of Active Sites

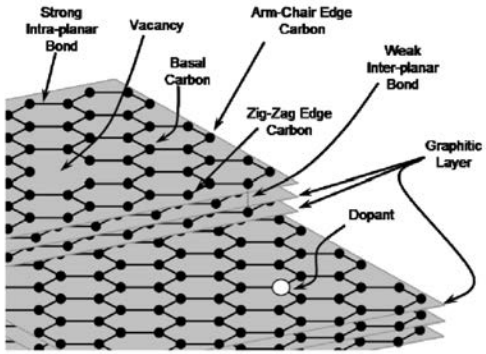

In temperature-programmed desorption (TPD) tests, chars are exposed to oxygen at low temperatures (673 K) for a long time, saturating the carbon sites with adsorbed oxygen atoms. The environment is switched to N_2 and the temperature is slowly ramped to ~ 1373 K. The off-gas is monitored for CO and CO_2 during the increase in temperature.

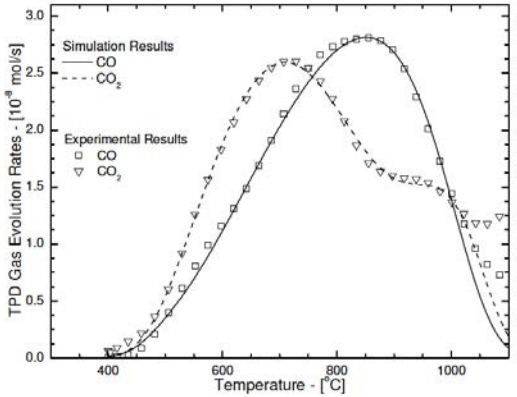

Rate of change in desorbing species concentration owing to activation energy distribution:

$$\frac{d[X_i]}{dt} = [X_i]_0 \int_0^{\infty} A\, exp(-E/\Re T) exp\left[-A \int_0^{t} exp(-E/\Re T)dt\right] \psi(E)dE$$

$$\psi(E) = \frac{1}{\sigma}\sqrt{\frac{1}{2\pi}}\, exp\left(-\frac{(E-E_{mean})^2}{2\sigma^2}\right)$$

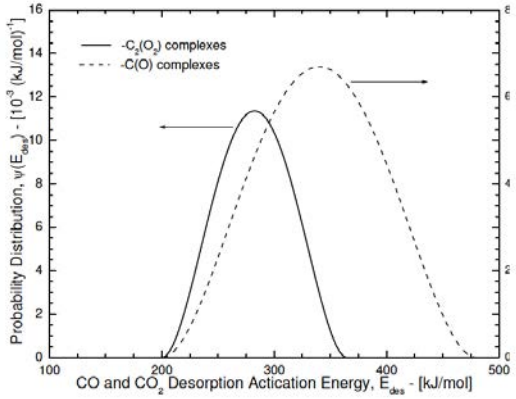

$$C_b + C(O) \longrightarrow CO + C_f$$

$$C_b + C_2(O_2) \longrightarrow CO_2 + 2\,C_f$$

A	E (kJ/mol)	σ
1.0 x 10^{13}	353	28
1.0 x 10^{13}	304	33

Kinetic Results for Synthetic Char

	Reaction	*A* (1/s, m^3/mol, m^2/mol)	*b*	*E* (kJ/mol)	*ω* (kJ/mol)	*a*
R8.1	-C + O_2 ⇄ -C-(O_2)	$k_f = 2.40 \times 10^5$	0.5	0	-	-
		$k_r = 1.15 \times 10^{14}$	-	50	-	-
R8.2	-C-(O_2) + -C → -C(O^m) + C(O^m)	8.73×10^{12}	-	137	60	1
R8.3	-C-(O_2) + -C → CO + C(O^m) + -C	1.00×10^{21}	-	310	150	1
R8.4	-C-(O_2) + -C → CO_2 + -C	2.61×10^{14}	-	154	150	10
R8.5	-C-(O_2) + -C(O) → CO + -C(O^m) + C(O^m)	3.94×10^{17}	-	206	-	-
R8.6	-C-(O_2) + -C(O) → CO_2 + -C(O^m) + -C	1.98×10^{17}	-	195	-	-
R8.7	-C(O^m) → -C(O)	1.00×10^{17}	-	23	-	-
R8.8	-C(O^m) + -C(O) → -C_2(O_2)	8.95×10^{11}	-	18	-	-
R8.9	-C(O) → -C(O^m)	3.98×10^{05}	-	200	-	-
R8.10	-C(O) → CO + -C	1.00×10^{13}	-	150, 480	-	-
R8.11	-C_2(O_2) → CO_2 + -C + -C	1.00×10^{13}	-	114, 365	-	-

Assuming Arrhenius-type dependency: $k = A\,T^b\,exp(-E/\Re T)$

Surface coverage dependency applies: $E = E_0(1-(1-\theta)^a)(\omega/a)$

Desorption activation energy distribution function:

$$\psi(E) = 30\,(E-E_{max})^2(E-E_{min})^2/(E_{max}-E_{min})^5$$

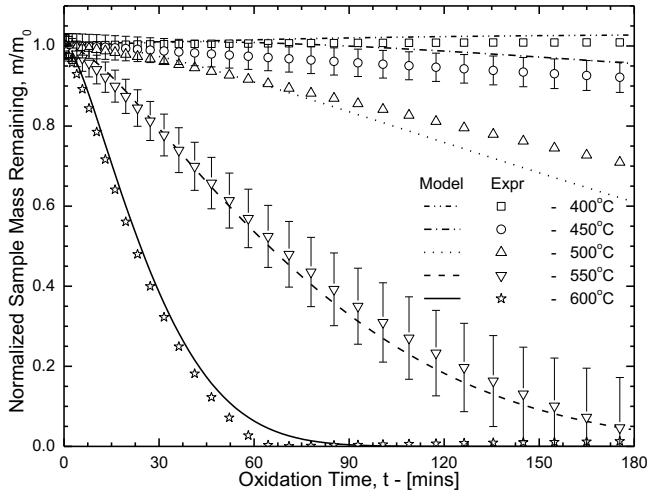

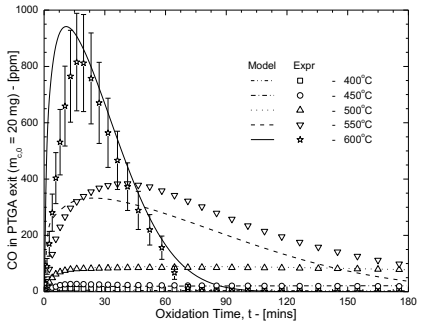

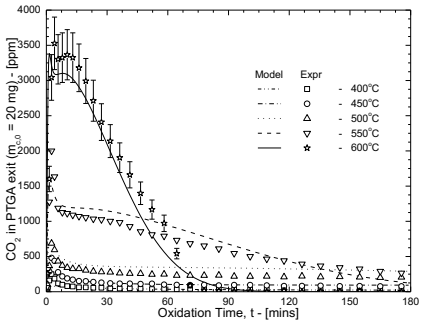

Oxidation Pathway Diagrams

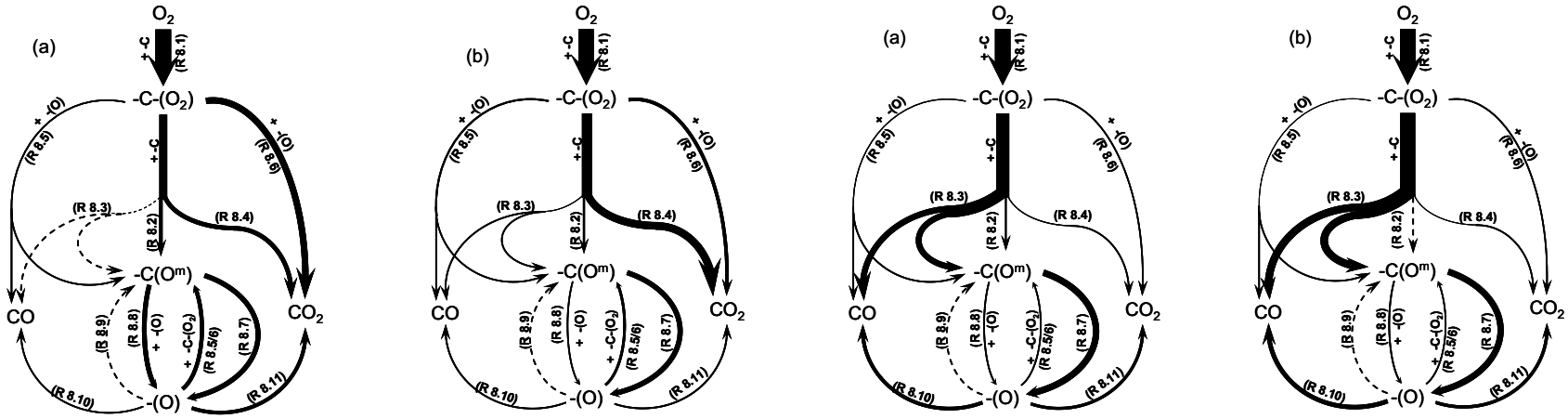

T=400 °C, P_{O2}=60 kPa | T=800 °C, P_{O2}=60 kPa | T=1200 °C, P_{O2}=60 kPa | T=1600 °C, P_{O2}=60 kPa

The widths of the arrows are approximately proportional to the flux of oxygen atoms between the specified chemical forms. Dashed arrows represent reactions of negligible magnitude.

For temperatures less than 800 °C, the char oxidation primarily results in CO_2 formation. The higher the oxidation temperature, the greater the fraction of carbon in CO.

Reduced Char Gasification and Combustion Mechanism

	Reaction	Reaction rate (mol/m^2-s)
R.1	$2C_f + H_2O \Leftrightarrow C(OH) + C(H)$	$\hat{R}_1 = (S/N_{AV})^2\{k_{1f}[H_2O]\theta_f^2 - k_{1r}\theta_{OH}\theta_H\}$
R.2	$C(OH) + C_f \Leftrightarrow C(O) + C(H)$	$\hat{R}_2 = (S/N_{AV})^2\{k_{2f}\theta_f\theta_{OH} - k_{2r}\theta_O\theta_H\}$
R.3	$C(H) + C(H) \Leftrightarrow H_2 + 2C_f$	$\hat{R}_3 = (S/N_{AV})^2\{k_{3f}\theta_H^2 - k_{3r}[H_2]\theta_f^2\}$
R.4	$C(O) + C_b \rightarrow CO + C_f$	$\hat{R}_5 = (S/N_{AV})k_5\theta_O$
R.5	$C(OH) + C_b \Leftrightarrow HCO + C_f$	$\hat{R}_6 = (S/N_{AV})\{k_{6f}\theta_{OH} - k_{6r}[HCO]\theta_f\}$
R.6	$C_b + C_f + C(H) + H_2O \Leftrightarrow CH_3 + C(O) + C_f$	$\hat{R}_7 = (S/N_{AV})^2\{k_{7f}[H_2O]\theta_f\theta_H - k_{7r}[CH_3]\theta_f\theta_O\}$
R.7	$C_b + C_f + C(H) + H_2 \Leftrightarrow CH_3 + 2C_f$	$\hat{R}_8 = (S/N_{AV})^2\{k_{8f}[H_2]\theta_f\theta_H - k_{8r}[CH_3]\theta_f^2\}$
R.8	$C_f + C(H) + CO \rightarrow HCO + 2C_f$	$\hat{R}_9 = (S/N_{AV})^2 k_{9f}[CO]\theta_f\theta_H$
R.9	$C(H) + C(H) \rightarrow CH_2 + C_f$	$\hat{R}_{10} = (S/N_{AV})^2 k_{10f}\theta_H^2$
R.10	$CO_2 + C_f \Leftrightarrow C(O) + CO$	$\hat{R}_{11} = (S/N_{AV})\{k_{11f}[CO_2]\theta_f - k_{11r}[CO]\theta_O\}$
R.11	$C_b + CO_2 + C(O) \rightarrow 2CO + C(O)$	$\hat{R}_{12} = (S/N_{AV})k_{12f}[CO_2]\theta_O$
R.12	$CO + C_f \Leftrightarrow C(CO)$	$\hat{R}_{13} = (S/N_{AV})\{k_{13f}[CO]\theta_f - k_{13r}\theta_{CO}\}$
R.13	$CO + C(CO) \rightarrow CO_2 + C_f + C_b$	$\hat{R}_{14} = (S/N_{AV})k_{14f}[CO]\theta_{CO}$
R.14	$2C_f + O_2 \rightarrow C(O) + CO$	$\hat{R}_{15} = (S/N_{AV})^2 k_{15f}[O_2]\theta_f^2$
R.15	$2C_f + O_2 \rightarrow C_2(O_2)$	$\hat{R}_{16} = (S/N_{AV})\{(S/N_{AV})k_{16f}[O_2]\theta_f^2 - k_{16r}\theta_{O2}\}$
R.16	$C_f + C_b + C(O) + O_2 \rightarrow CO_2 + C(O) + C_f$	$\hat{R}_{17} = (S/N_{AV})^2\{k_{17f}[O_2]\theta_f\theta_O - k_{17r}[CO_2]\theta_f\theta_O\}$
R.17	$C_f + C_b + C(O) + O_2 \rightarrow CO + 2C(O)$	$\hat{R}_{18} = (S/N_{AV})^2 k_{18f}[O_2]\theta_f\theta_O$
R.18	$C_b + C_2(O_2) \rightarrow CO_2 + 2C_f$	$\hat{R}_{19} = (S/N_{AV})k_{19f}\theta_{O2}$

$$R_{iC,H2O} = \hat{M}_C\left\{\hat{R}_4 + \hat{R}_5 + \hat{R}_6 + \hat{R}_7 + \hat{R}_9\right\}$$

$$\left(\frac{1}{m_C}\frac{dm_C}{dt}\right)_{H_2O} = -S_g R_{iC,H2O}$$

$$R_{iC,CO2} = \hat{M}_C\left\{\hat{R}_4 + \hat{R}_{11} - \hat{R}_{13}\right\}$$

$$\left(\frac{1}{m_C}\frac{dm_C}{dt}\right)_{CO_2} = -S_g R_{iC,CO_2}$$

$$R_{iC,O2} = \hat{M}_C\left\{\hat{R}_4 + \hat{R}_{14} + \hat{R}_{16} + \hat{R}_{17} + \hat{R}_{18}\right\}$$

$$\left(\frac{1}{m_C}\frac{dm_C}{dt}\right)_{O_2} = -S_g R_{iC,O2}$$

Reaction Rate Coefficients and Thermochemistry

Generic chemical reaction: $(\mathrm{a}A + bB \rightleftharpoons cC + dD)$

- Forward reaction rate coefficients are adjusted to fit mass loss data.
- Reverse reaction rate coefficients are determined from equilibrium and thermodynamic relations.

$$k_r = \frac{k_f}{K_C} \qquad K_C = K_P \left(\frac{P_{ref}}{RT}\right)^{(c+d-a-b)}$$

$$K_P = \exp\left(-\frac{\Delta G_R}{RT}\right) \qquad \Delta G_R = \Delta H_R - \mathrm{T}\,\Delta S_R$$

- Enthalpies of formation and absolute entropies for adsorbed species were treated as unknowns and adjusted along with Arrhenius parameters to fit mass loss data.

Heat of formation

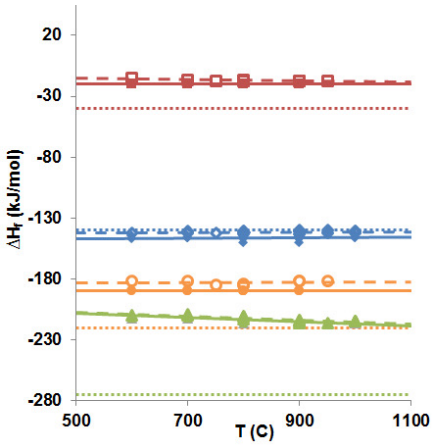

Absolute entropy

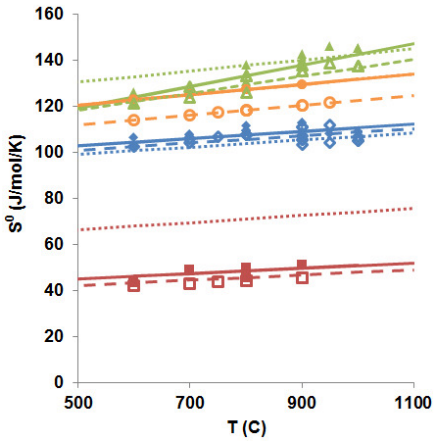

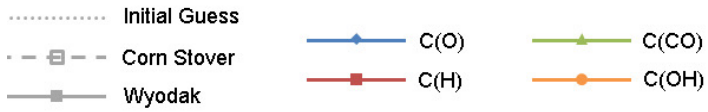

Kinetic Parameters for Rate Coefficients

		Wyodak coal char			Corn Stover char		
	Reaction	**Pre-Exponential *A***	**Activation Energy *E*** (kJ/mol)	**Std Dev σ** (kJ/mol)	**Pre-Exponential *A***	**Activation Energy *E*** (kJ/mol)	**Std Dev σ** (kJ/mol)
R.1	$2C_f + H_2O \Leftrightarrow C(OH) + C(H)$	$2.1 \cdot 10^{6}$	105	--	$7.3 \cdot 10^{7}$	106	--
R.2	$C(OH) + C_f \Leftrightarrow C(O) + C(H)$	$4.1 \cdot 10^{11}$	80	--	$1.5 \cdot 10^{12}$	150	--
R.3	$C(H) + C(H) \Leftrightarrow H_2 + 2C_f$	$1.4 \cdot 10^{11}$	67	--	$1.0 \cdot 10^{12}$	100	--
R.4	$C(O) + C_b \rightarrow CO + C_f$	$1.0 \cdot 10^{13}$	353	28	$1.0 \cdot 10^{13}$	353	28
R.5	$C(OH) + C_b \Leftrightarrow HCO + C_f$	$1.0 \cdot 10^{13}$	393	28	$1.0 \cdot 10^{13}$	393	28
R.6	$C_b + C_f + C(H) + H_2O \Leftrightarrow CH_3 + C(O) + C_f$	$1.0 \cdot 10^{13}$	300	--	$1.0 \cdot 10^{13}$	300	--
R.7	$C_b + C_f + C(H) + H_2 \Leftrightarrow CH_3 + 2C_f$	$1.0 \cdot 10^{13}$	300	--	$1.0 \cdot 10^{13}$	300	--
R.8	$C_f + C(H) + CO \rightarrow HCO + 2C_f$	$1.0 \cdot 10^{13}$	300	--	$1.0 \cdot 10^{13}$	300	--
R.9	$C(H) + C(H) \rightarrow CH_2 + C_f$	$3.0 \cdot 10^{11}$	426	--	$3.0 \cdot 10^{11}$	426	--
R.10	$CO_2 + C_f \Leftrightarrow C(O) + CO$	$3.7 \cdot 10^{3}$	161	--	$8.6 \cdot 10^{4}$	188	--
R.11	$C_b + CO_2 + C(O) \rightarrow 2CO + C(O)$	$1.26 \cdot 10^{8}$	276	--	$3.26 \cdot 10^{12}$	367	--
R.12	$CO + C_f \Leftrightarrow C(CO)$	$1.0 \cdot 10^{13}$	455	53	$1.0 \cdot 10^{13}$	455	53
R.13	$CO + C(CO) \rightarrow CO_2 + 2C_f$	$9.8 \cdot 10^{6}$	270	--	$3.36 \cdot 10^{6}$	266	--
R.14	$2C_f + O_2 \rightarrow C(O) + CO$	$5.0 \cdot 10^{10}$	150	--	$7.0 \cdot 10^{10}$	150	--
R.15	$2C_f + O_2 \rightarrow C_2(O_2)$	$4.0 \cdot 10^{7}$	93	--	$3.0 \cdot 10^{8}$	103	--
R.16	$C_f + C_b + C(O) + O_2 \rightarrow CO_2 + C(O) + C_f$	$1.5 \cdot 10^{7}$	78	--	$1.5 \cdot 10^{7}$	78	--
R.17	$C_f + C_b + C(O) + O_2 \rightarrow CO + 2C(O)$	$2.1 \cdot 10^{7}$	103	--	$2.1 \cdot 10^{7}$	103	--
R.18	$C_b + C_2(O_2) \rightarrow CO_2 + 2C_f$	$1.0 \cdot 10^{13}$	304	33	$1.0 \cdot 10^{13}$	304	33

Calculated and Measured Normalized Mass Loss Rates in O_2

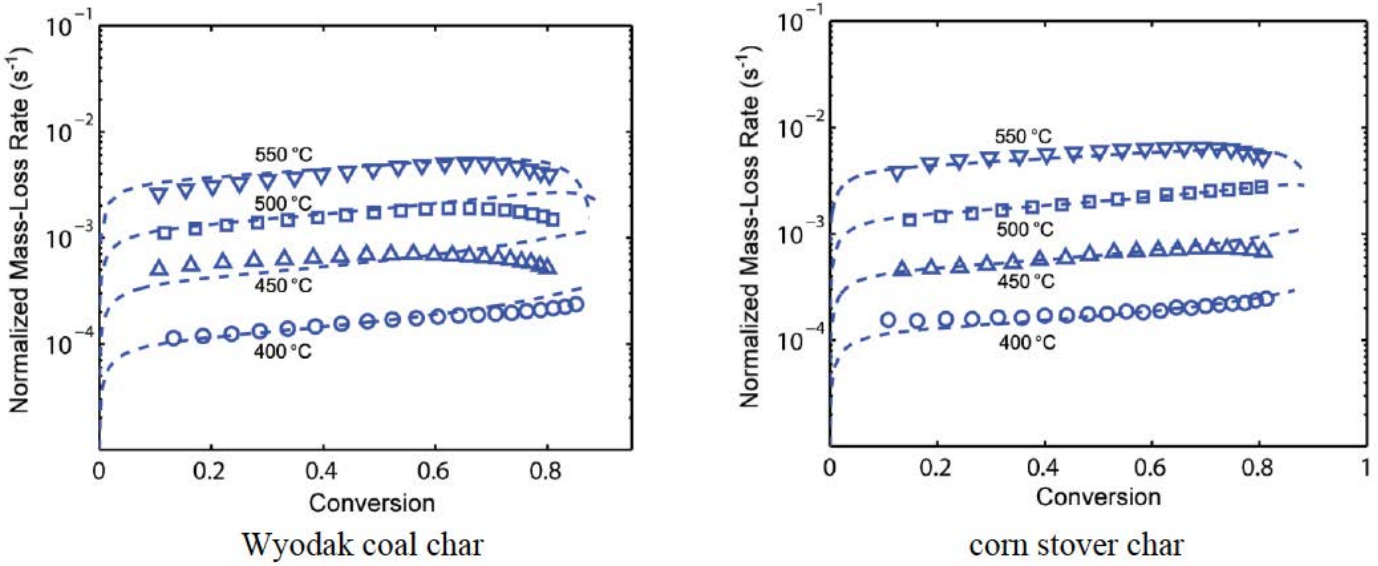

Wyodak Coal and corn stover char particles exposed to 6% oxygen at 1 atm and selected temperatures.

Calculated and Measured Normalized Mass Loss Rates in CO_2

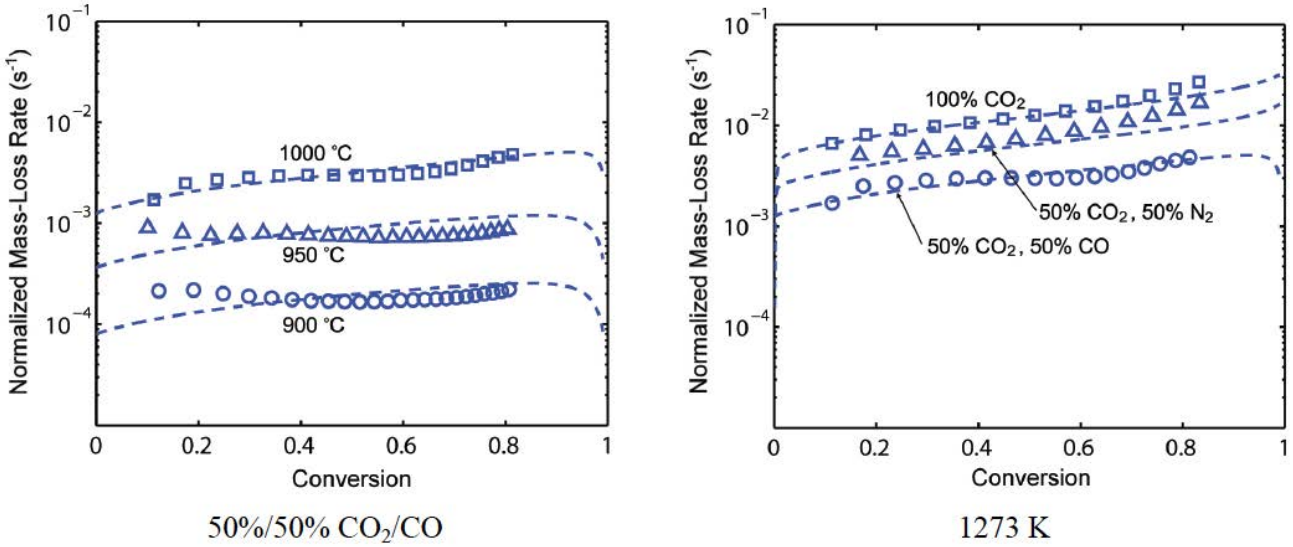

Wyodak coal char particles exposed to selected environments containing CO_2, CO and N_2 at 1 atm and selected temperatures.

Calculated and Measured Normalized Mass Loss Rates in H_2O

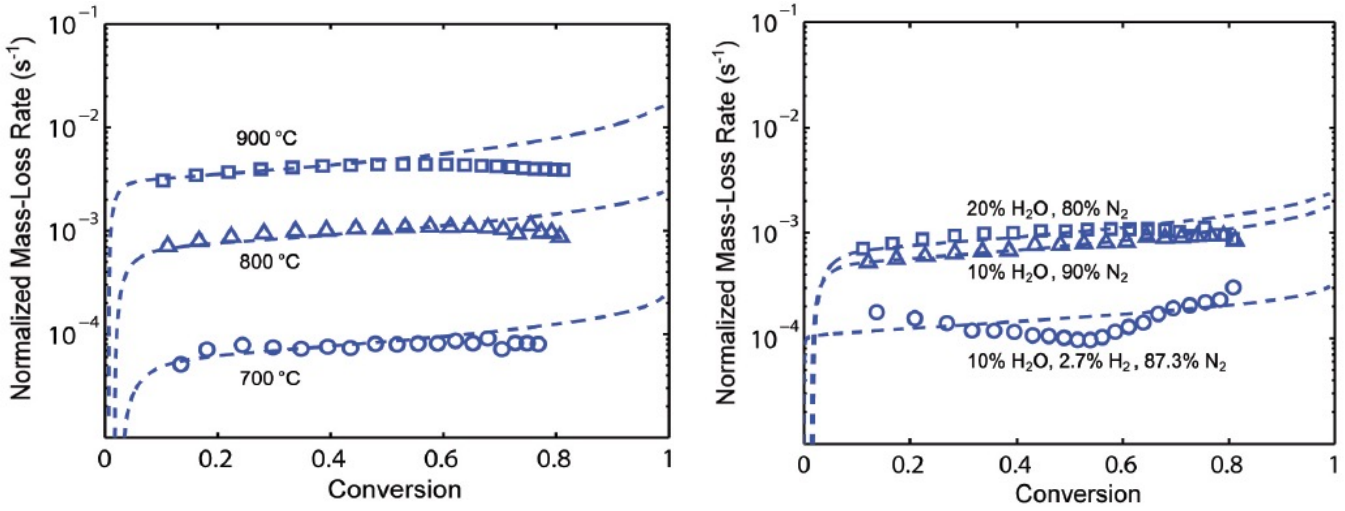

Wyodak coal char particles exposed to (left) 20% steam (balance N_2) at 1 atm and selected temperatures and (right) selected $H_2O/H_2/N_2$ mixtures at 900 ° C.

Carbon-Based Solid Oxide Fuel Cells

Development of a solid oxide electrolytic cell for the production of both power and hydrogen by coupling a steam-carbon cell to an air-carbon cell.

Research Collaborator: Professor Turgut Gür
Graduate Students: Andrew Lee, Brentan Alexander, David Johnson, Kevin Steinberger

The Air-Carbon Fuel Cell

In an air-carbon fuel cell, the chemical potential difference between carbon and oxygen is utilized to extract electrical work in an electrochemical cell.

In operation, oxygen ions migrate through an impervious, electronically insulating but ionically conducting yttria-stabilized zirconia (YSZ) electrolyte.

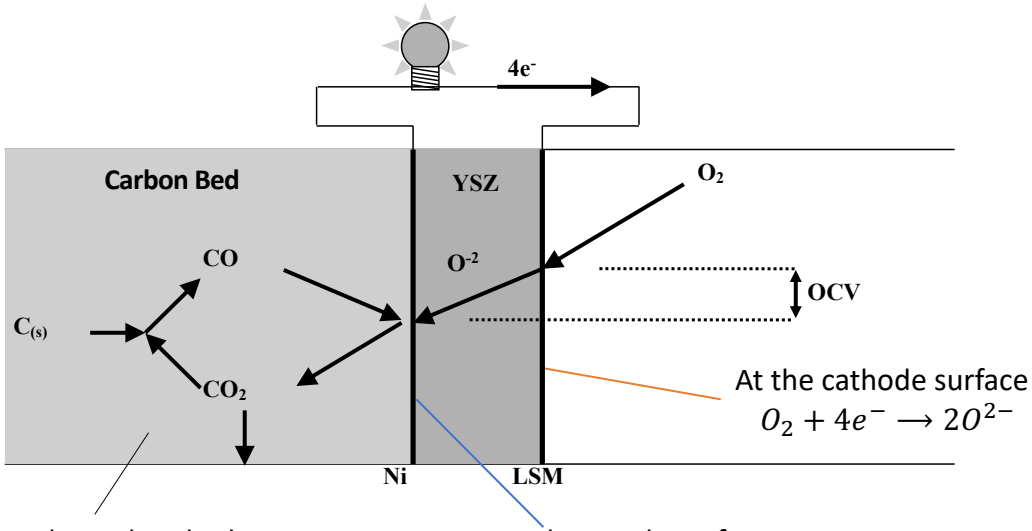

At the cathode surface

$O_2 + 4e^- \longrightarrow 2O^{2-}$

In the carbon bed

$CO_2 + C \longrightarrow 2CO$

(the Boudouard reaction)

At the anode surface

$2CO + 2O^{2-} \longrightarrow 2CO_2 + 4e^-$

Overall reaction for an air-carbon fuel cell:

$$C + O_2 \longrightarrow CO_2$$

When the combustion reaction is carried out in the air-carbon fuel cell, 4 electrons are circulated through the external circuit for each carbon atom consumed in the bed.

The Air-Carbon Fuel Cell

The performance with the CO_2-gasified carbon particles compares well with the performance of the same cell operating on pure CO.

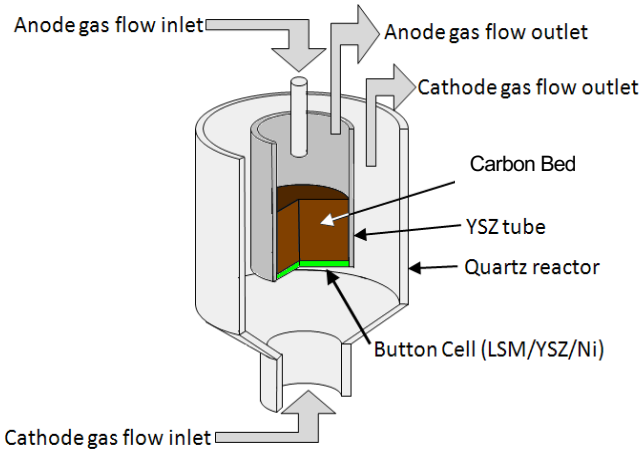

Anode: Nickel cermet
Cathode: LSM-YSZ composite
Active electrode area: ~0.18 cm^2

LSM = Lanthanum strontium manganate

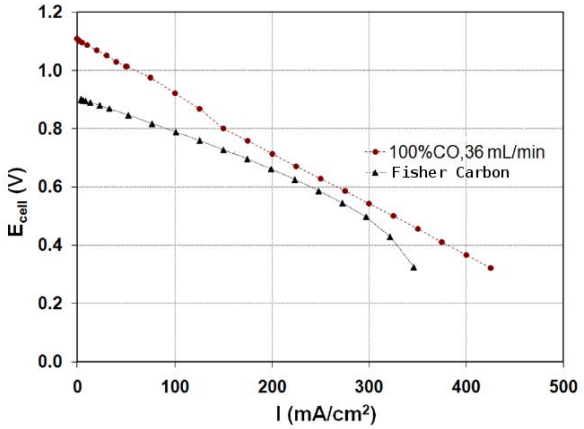

Measured polarization performance for a button cell operating in a fluidized bed with carbon particles fluidized by CO_2 at 900 °C. Also, shown or comparison, in the same cell operating on pure CO.

Air-Carbon Fuel Cell Performance

Polarization performance with gasified synthetic carbon at 900 °C on 5-cm^2 active electrode area in anode supported YSZ.

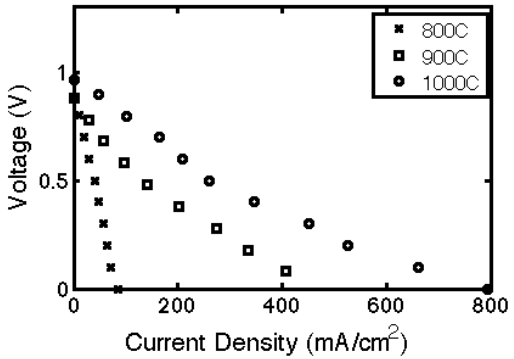

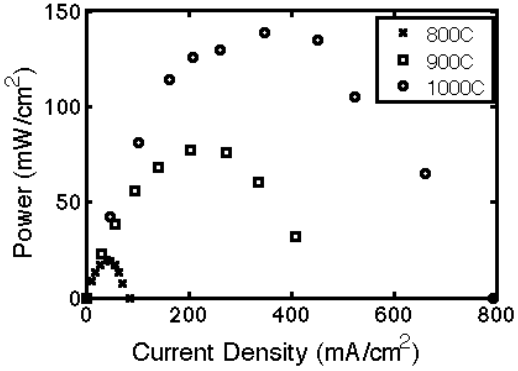

Ultimate Analysis of Synthetic Char

Moisture, %	1.22
Ash, %	2.45
Carbon, %	80.90
Hydrogen, %	3.04
Nitrogen, %	0.66
Sulfur, %	0.31
Oxygen, % (by diff)	11.42

Polarization performance with gasified biomass particles at 900 °C with ~0.2-cm^2 active electrode area.

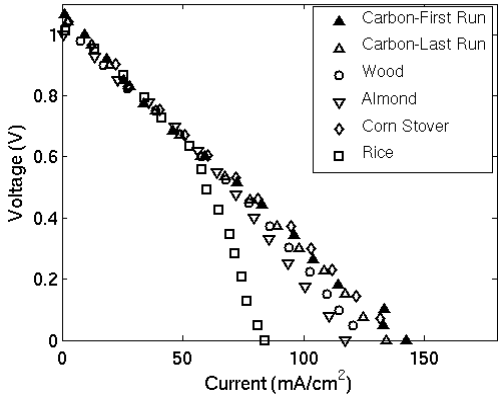

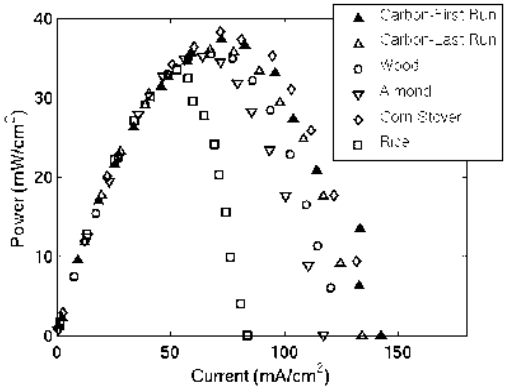

Modeling Carbon Fuel Cells

Finite-element models of a planar, button-type carbon-air fuel cell and an axi-symmetric, tubular carbon-air fuel were developed to determine the relationship between overall cell efficiency, hydrogen production rate, and electricity production.

The models include

- Cell Electrochemistry
  - Nernst equation to calculate the open circuit voltage
  - Ohm's Law to predict the over-potential of the electrolyte
  - Butler-Volmer equation to describe activation losses at the anode and cathode surfaces
- Mass Transport
  - Convection and diffusion
  - Darcy's law (porous media)
- Carbon bed chemistry of dry gasification

  (Boudouard reaction)
- Heat Transfer
  - Gas phase convection/conduction
  - Wall-to-wall radiation
  - Fuel bed convection, conduction, and radiation

Planar geometry

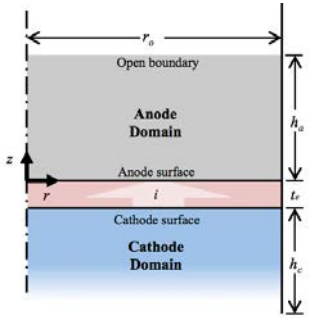

Tubular geometry

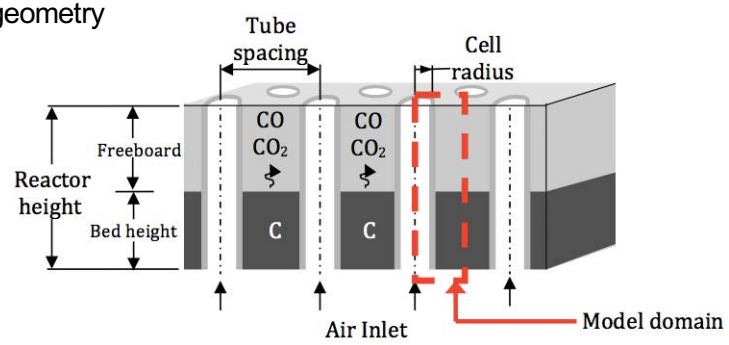

Representative CFC Model Results

Model Input: V_{cell} = 0.7 V, h = 5 cm, tube spacing = 5 cm

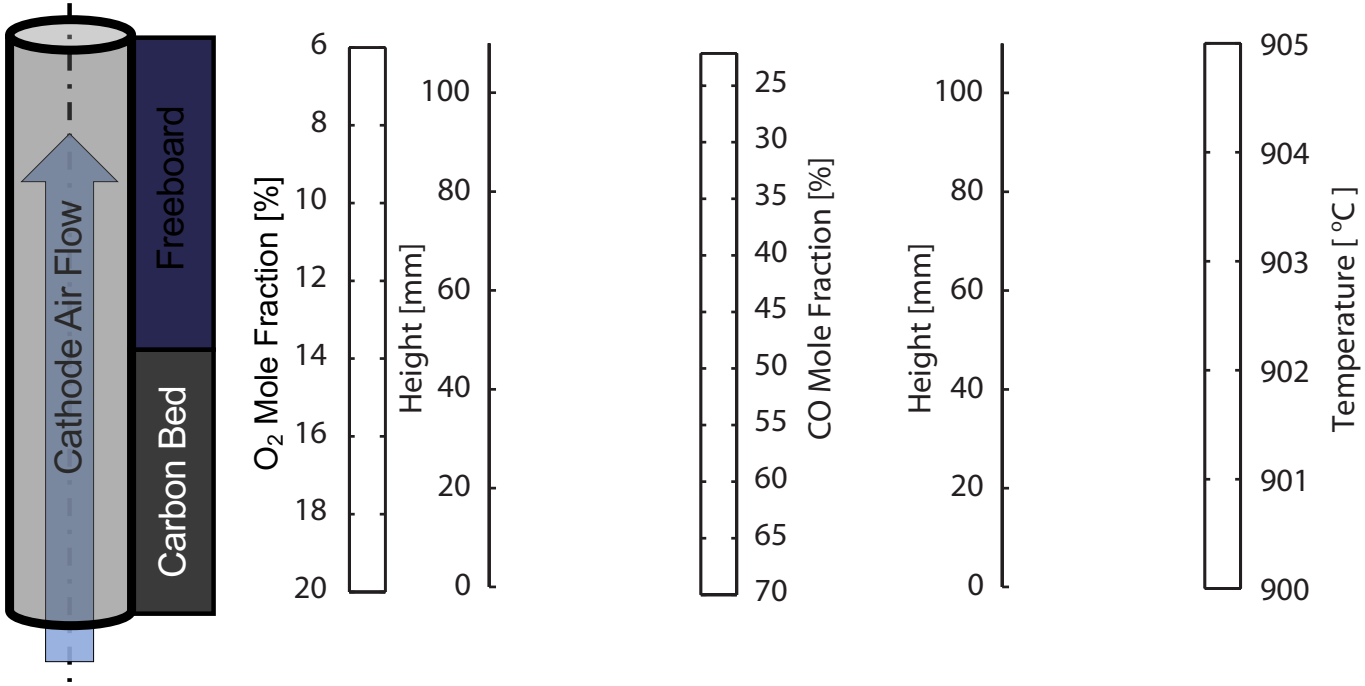

Predicting Carbon Fuel Cell Performance

- Independent variables: carbon bed height, freeboard height, tube spacing, and the cell voltage.
- Calculated output: power density and cell efficiency

$$P = \frac{V_{cell}}{A}\int jdA$$

$$\eta_{cell} = \frac{PA}{\dot{m}_{char} HHV_{char}}$$

Power density as a function of bed height and tube spacing at a fixed cell voltage of 0.7 V

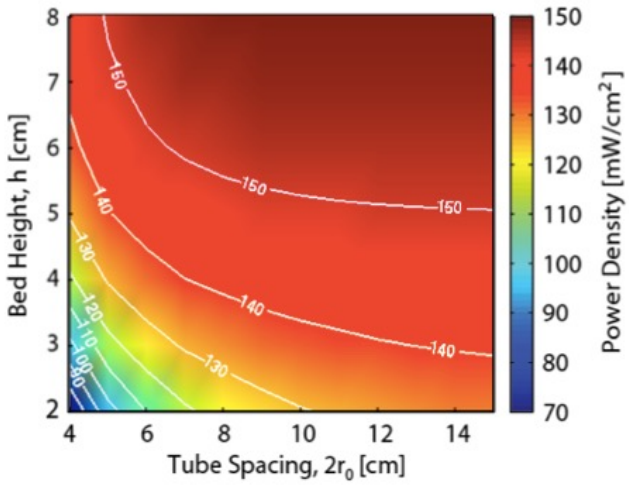

Cell efficiency as a function of bed height and tube spacing at a fixed cell voltage of 0.7 V

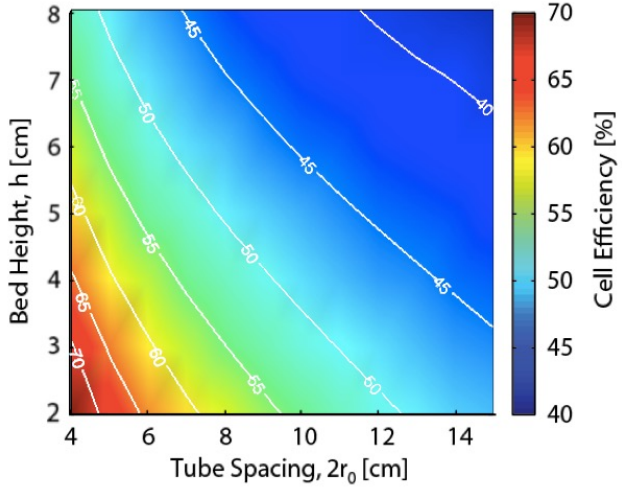

The Steam-Carbon Fuel Cell

Water/Steam electrolysis is energetically uphill by > 0.9 V (*i.e., requires an external driving force*).

Chemically assisted water splitting is achieved without external electrical power.

The steam-carbon fuel cell eliminates the barrier with carbon chemistry at anode.

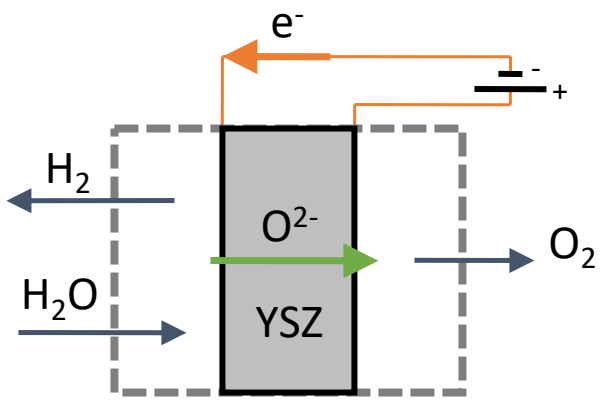

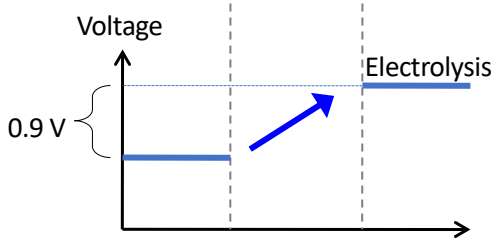

Overall reaction

$2H_2O \rightarrow 2H_2 + O_2$

$\Delta g(1173K) = 174 \frac{kJ}{molH_2}$

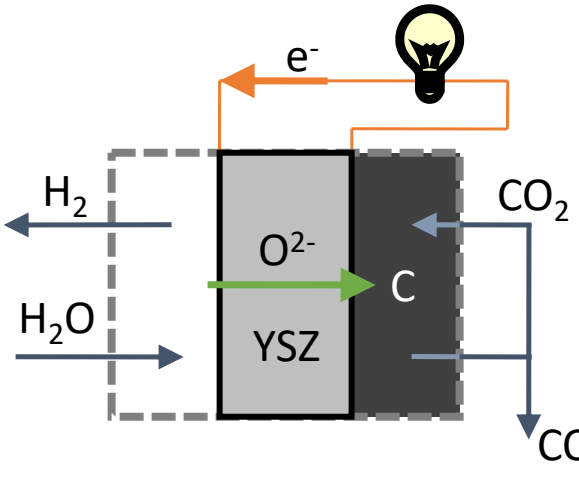

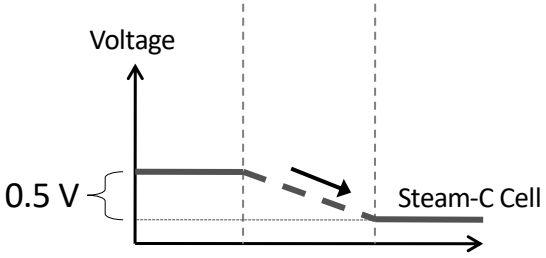

Overall reaction

$CO + H_2O \rightarrow H_2 + CO_2 \quad \Delta g(1173\ K) = -116 \frac{kJ}{molH_2}$

The Steam-Carbon Cell Results

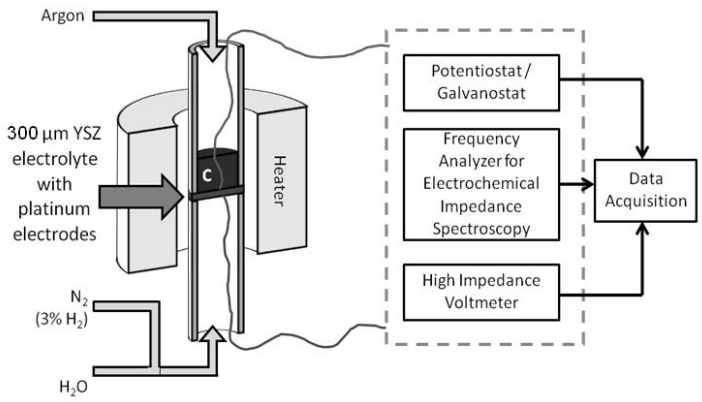

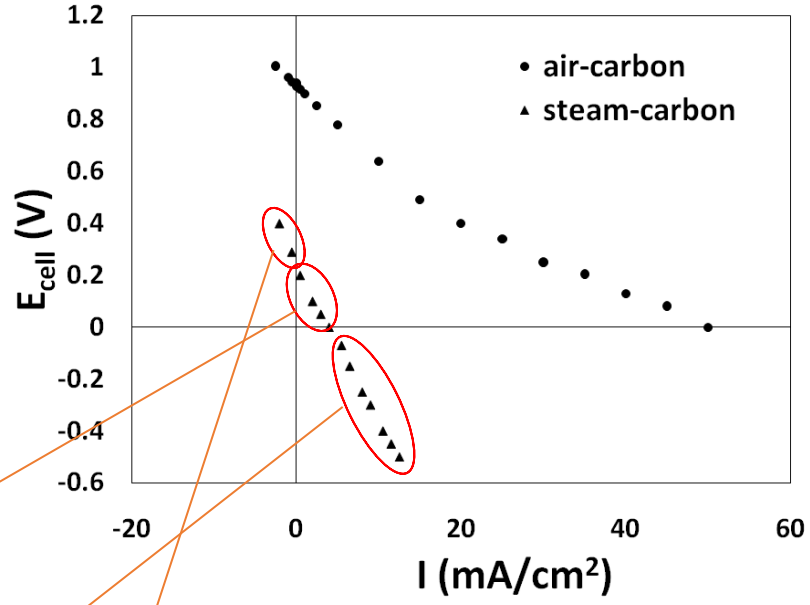

A positive cell potential and current represent fuel cell behavior and spontaneous hydrogen production: Spontaneous O from H_2O to C.

When the cell potential becomes negative, for a positive current, there is work input into the cell to force higher rates for oxygen transport: Forced O from H_2O to C.

Conversely, if the cell is operated under negative currents for a positive potential, oxygen is forced from the carbon bed to the steam side: Forced O from C to H_2O.

Characterizing Fuel Cell Behavior

Alternating current (AC) impedance spectroscopy was performed on cells to help identify cell loss mechanisms. Tests were conducted using a sinusoidal AC signal with V_{RMS} amplitude of 20 mV and frequencies ranging from 0.5 to 50,000 Hz. Impedance spectra were measured at cell operating temperatures ranging from 600 to 900 °C.

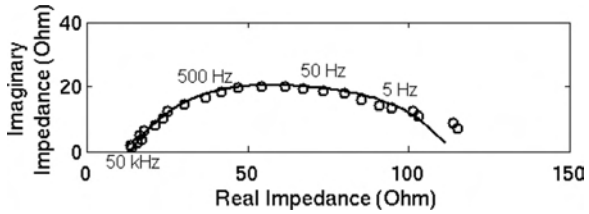

Representative EIS response to a steam-carbon cell operating at 850 °C at a cell voltage of 0.8 V along with fits (line) to the impedance spectra. The fits yield values for the resistances R_e, R_c, and R_a in the equivalent circuit.

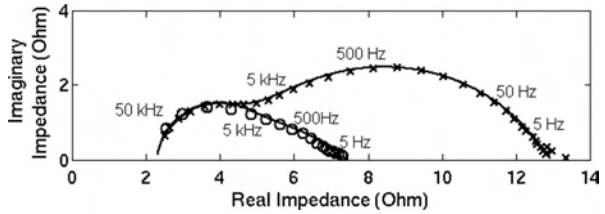

Representative EIS response to an air-carbon cell operating at 825 °C at cell voltages of 0.62 V (x) and 0.37 V (o), along with fits (line) to the impedance spectra employing the equivalent circuit.

An equivalent circuit model of the cell was employed to describe and fit the experimentally measured impedance spectra.

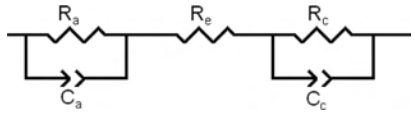

The cell current through the cell was monitored during each AC impedance test and combined with the resistance values extracted from the EIS data at the test temperatures to determine activation overvoltages in the Butler-Volmer relation ($i = i_0\{e^{\alpha nF/RT\eta} - e^{(\alpha-1)nF/RT\eta}\}$). This permits the prediction of cell voltage for a specified cell current at selected cell operating temperatures.

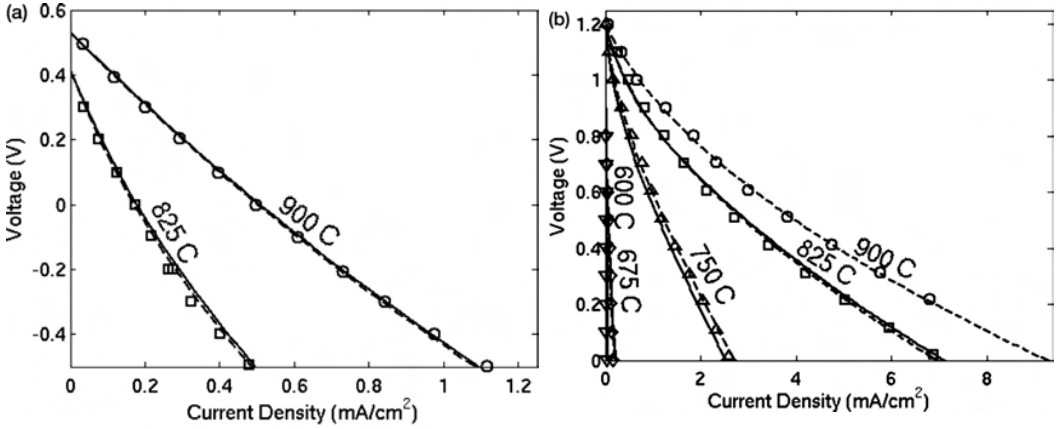

Predicted and experimental current-voltage behavior for (a) a steam-carbon fuel cell and (b) an air-carbon fuel cell.

Coupled Steam-Carbon and Air-Carbon Fuel Cells

- We have demonstrated our steam-carbon and air-carbon SOFC that produces electricity and can use a variety of carbons as the resource. YSZ is used as the membrane.

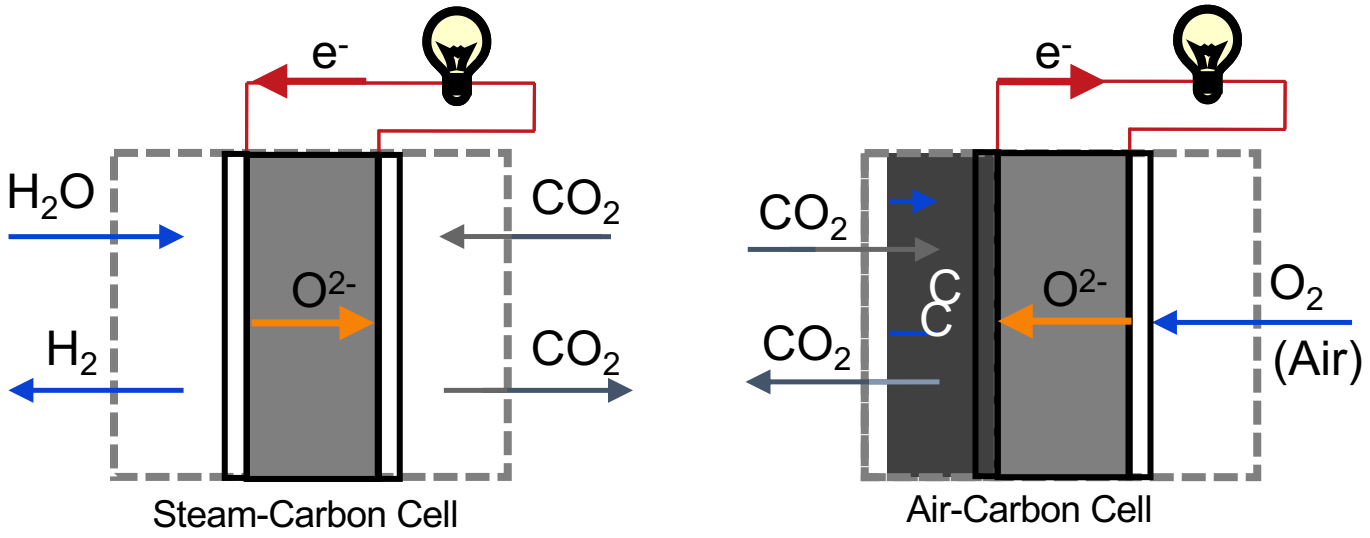

Coupled Steam-Carbon and Air-Carbon Fuel Cells

- We are now coupling the cells to form a steam-carbon/air-carbon electrochemical cell that permits simultaneous production of H_2 and electricity.

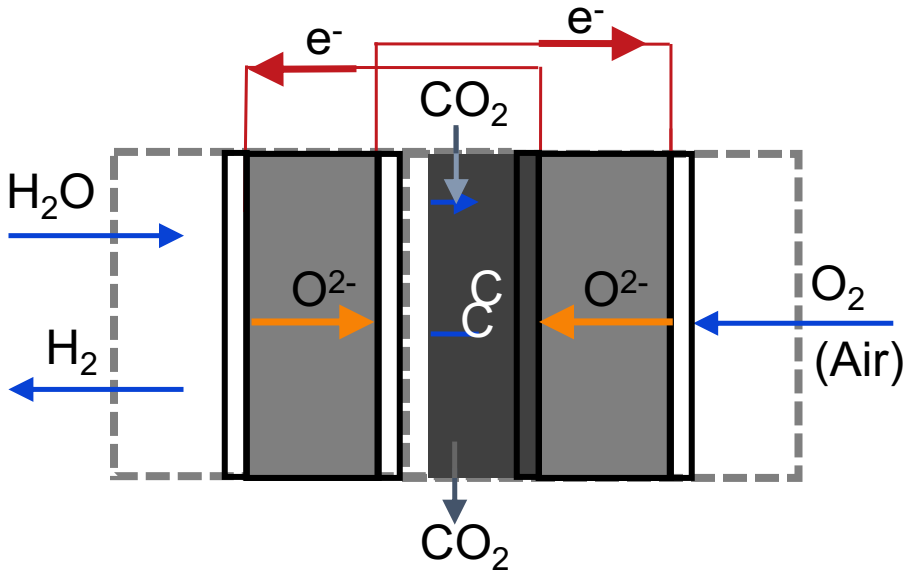

This coupled cell is capable of spontaneously generating both hydrogen and electricity.

Steam-Carbon Cell

Air-Carbon Cell

Coupled Steam-Carbon-Air Carbon Cell

By coupling the air-carbon cell with the steam-carbon cell, a novel device that produces both hydrogen and electricity spontaneously without the need for external heat or power input is realized.

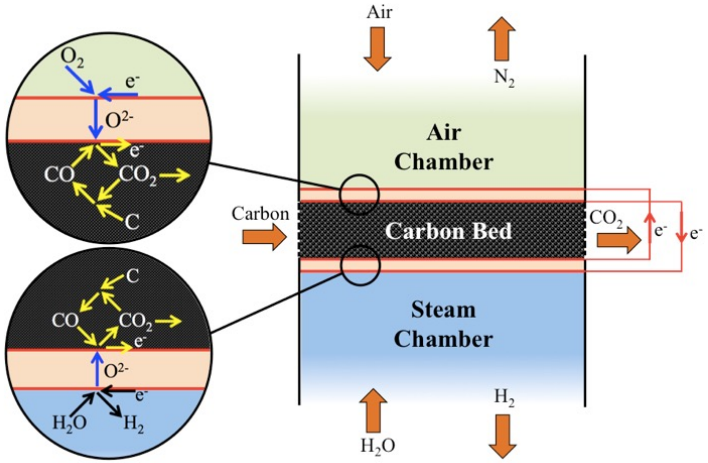

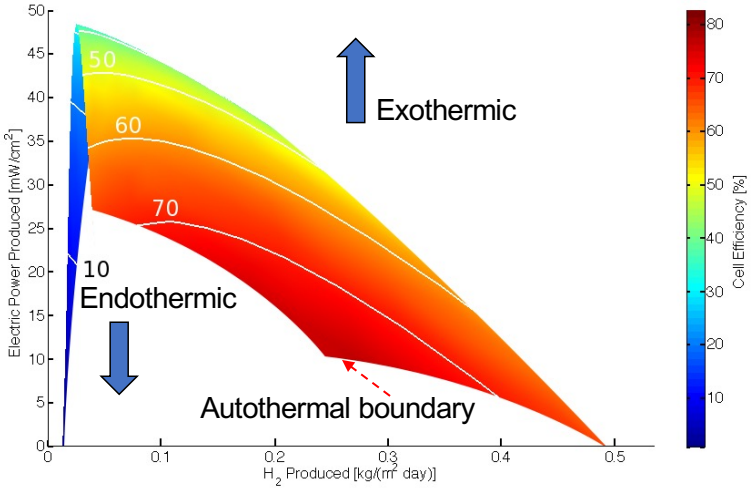

A finite element model of the coupled system was developed to determine the relationship between overall cell efficiency, hydrogen production rate, and electricity production. The model includes cell electrochemistry, carbon bed chemistry, and heat and mass transport throughout the system.

$$\eta = \frac{P_{out} + \dot{m}_{H_2} \cdot HHV_{H_2}}{\dot{m}_{char} \cdot HHV_{char} + P_{in} + Q_{in}}$$

Hydrogen – A Carbon-Free Fuel

CO_2 is a Greenhouse Gas

The greenhouse effect occurs when greenhouse gases in the Earth's atmosphere trap some of the heat radiated from the Earth's surface. The heat-trapping gases, in effect, act as a blanket that is wrapped around the Earth, keeping the Earth warmer than it would be without them.

A greenhouse gas (GHG) is a gas that absorbs and emits radiant energy at thermal infrared wavelengths (between 8 and 15 μm) , causing the greenhouse effect. Most of the energy in this wavelength range is emitted by the Earth as heat. Common GHGs are carbon dioxide, methane, nitrous oxide, and water vapor.

- The greenhouse gases that occur naturally in the Earth's atmosphere keep Earth at 15 °C, on average.
- If there were no CO_2 in the Earth's atmosphere, the surface of the Earth would be about 33 °C cooler.
- The level of CO_2 in the Earth's atmosphere has been rising (owing to the use of fossil fuels to meet our energy needs), trapping extra energy as heat near Earth's surface, causing temperatures to rise.

All our common fuels (coal, oil & natural gas) contain C, H, and O atoms, and when burned form CO_2 and H_2O.

When using these fuels to meet our energy needs, the CO_2 must be captured and stored to prevent future increases in the temperature of the Earth.

We could use a fuel that contains no carbon atoms.

Hydrogen – The Fuel of the 21st Century

Coal was the fuel of the 19th Century Natural gas was the fuel of the 20th Century

Hydrogen will be the fuel of the 21st Century

The problem: Hydrogen in molecular (H_2) form is scarcely present in Nature therefore, it must be obtained from primary energy sources that do occur naturally in Nature.

Water is the main source of hydrogen, however, the large amount of energy needed to split water (electrolysis) is a serious limitation.

The hydrogen in such renewables as biomass, algae, food waste, and municipal solid waste can be obtained via gasification and fermentation processes.

The hydrogen in methane can be obtained via methane pyrolysis.

The hydrogen in methane, natural gas and bio-oils can be obtained via reforming processes.

The hydrogen in coal and biomass can be obtained via gasification processes.

Electrolysis, pyrolysis, reforming, gasification, and fermentation are present-day methods of producing hydrogen from our primary energy sources.

The Colors of Hydrogen

White hydrogen

- Refers to naturally occurring hydrogen in its most natural state. It is generated by a natural process inside the Earth's crust.

Green hydrogen

- Produced primarily by splitting water using electricity generated from renewable energy sources (*e.g.*, wind, solar, hydroelectric)
- No CO_2 emissions are associated with this type of hydrogen production nor with its usage

Pink/Red/Purple hydrogen

Generated by splitting water using nuclear energy

- Pink hydrogen is generated through the electrolysis of water
- Red hydrogen is generated through the high-temperature catalytic splitting of water
- Purple hydrogen is generated using nuclear power and heat through combined chemothermal electrolysis of water.

Yellow hydrogen

- Hydrogen generated from electrolysis with electricity from the available grid power.

Blue hydrogen

- Derived from natural gas
- CO_2 emitted during the process is captured and stored

Turquoise hydrogen

- Produced via methane pyrolysis
- Solid carbon is a by-product that is used as a raw material (*e.g.,* in the production of car tires, plastics and batteries.

Grey hydrogen

- Derived from fossil fuels primarily via steam methane reforming
- CO_2 is released to the atmosphere.

Black/Brown hydrogen

- Produced from a type of bituminous coal (black) or lignite (brown)
- CO_2 and CO are released to the atmosphere.

Water Electrolysis

Overall chemical reaction

$$H_2O \longrightarrow 0.5\ O_2 + H_2$$

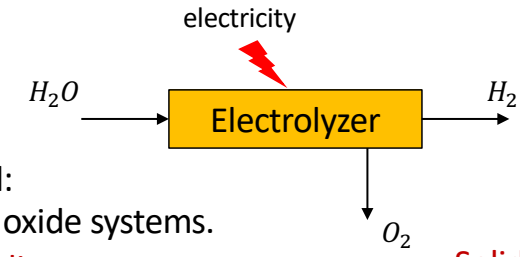

For clean hydrogen, grid electricity must be generated via renewables.

Three technologies for electrolysis are well-developed:
Proton exchange membrane (PEM), alkaline and solid oxide systems.

PEM

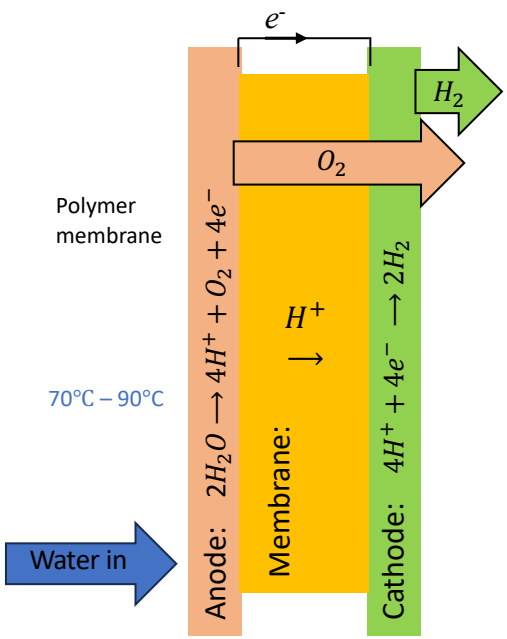

Alkaline

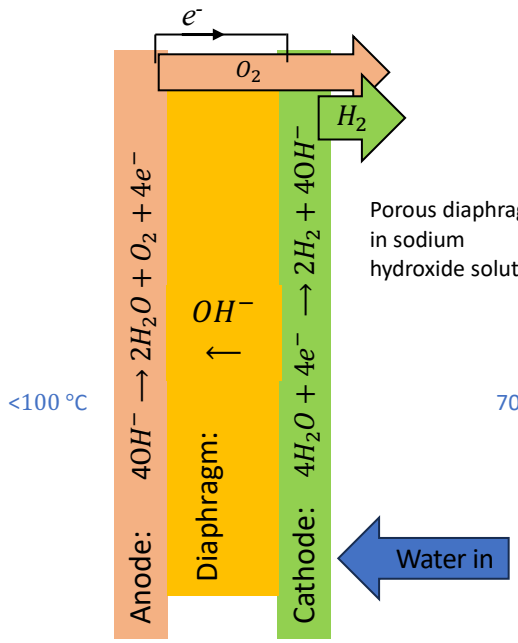

Solid Oxide

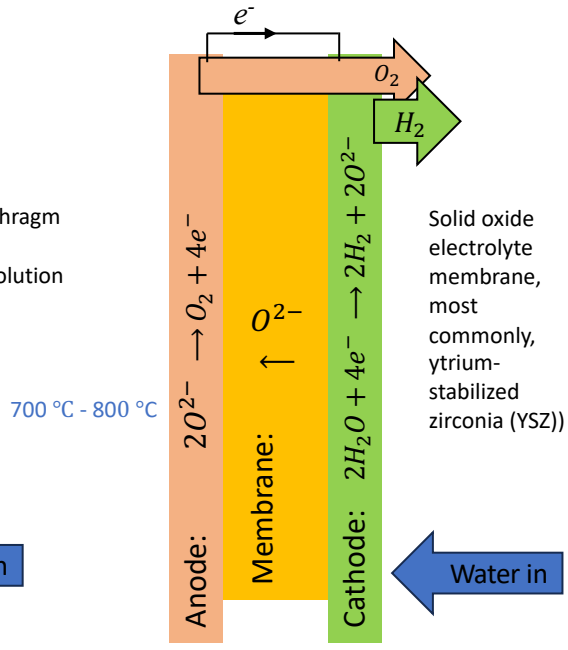

Methane Pyrolysis

Methane pyrolysis chemical reaction

$$CH_4 \longrightarrow C + 2\,H_2$$

Without a catalyst, the thermal decomposition of methane requires temperatures in excess of 1000 °C to achieve relevant reaction rates and methane conversions.

Nickel, iron and cobalt have been found to promote methane pyrolysis at relatively modest temperatures (~ 700 °C), with activity exhibiting the following trend: Ni > Co > Fe.

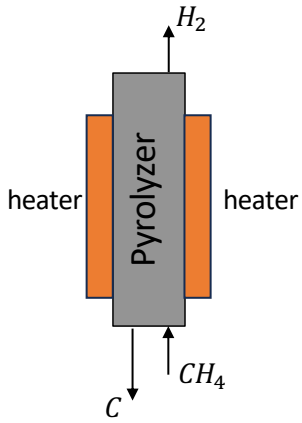

For clean hydrogen, energy supplied as heat must be generated via renewables.

Natural Gas Steam Reforming

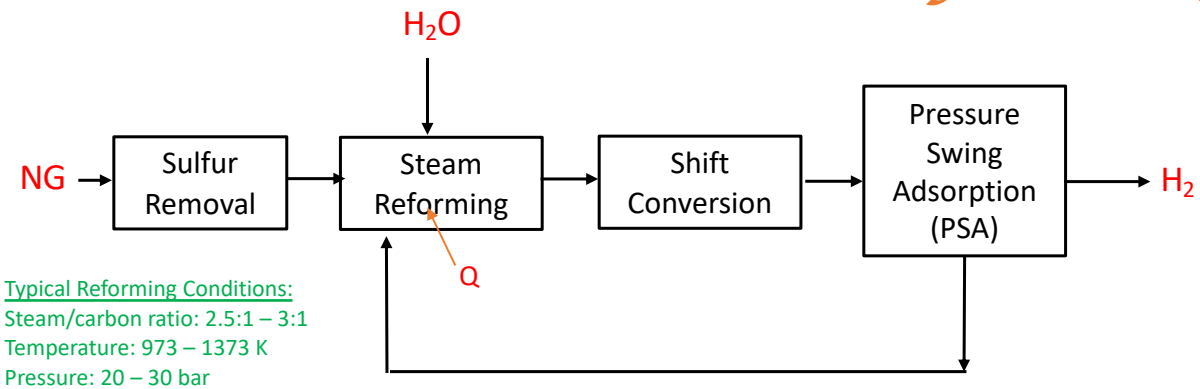

Typical Reforming Conditions:
Steam/carbon ratio: 2.5:1 – 3:1
Temperature: 973 – 1373 K
Pressure: 20 – 30 bar

Reforming reactions

$$C_nH_m + n\,H_2O \rightleftarrows n\,CO + \left(\frac{2n+m}{2}\right) H_2$$

$$CH_4 + H_2O \rightleftarrows CO + 3\,H_2$$

Water-Gas Shift reaction

$$CO + H_2O \rightleftarrows CO_2 + H_2$$

Natural Gas composition (wt-%)

Species	Formula	Mole-%
methane	CH4	93.037
ethane	C2H6	3.7
propane	C3H8	0.9
n-butane	nC4H10	0.13
i-butane	iC4H10	0.29
pentane	iC5H12	0.07
benzene	C6H6	0.07
sulfur dioxide	H2S	0.02
carbon dioxide	CO2	1.1
nitrogen	N2	0.68
oxygen	O2	0.001
helium	He	0.001
argon	Ar	0.001

Syngas composition:
Steam reforming at
1 atm, 1200 K

Species	kmol/s	mole fraction
CO	5.94E-02	2.51E-01
CO2	4.88E-04	2.06E-03
H2	1.73E-01	7.32E-01
H2O	1.96E-03	8.29E-03
H2S	1.15E-08	4.84E-08
SO2	1.19E-17	5.01E-17
HCl	1.00E-12	4.22E-12
Cl2	7.51E-33	3.17E-32
O2	4.77E-21	2.02E-20
N2	3.89E-04	1.64E-03
NH3	1.18E-06	4.98E-06
COS	1.24E-10	5.25E-10
CH4	1.19E-03	5.03E-03
He + Ar	1.15E-06	4.84E-06

Pressure swing adsorption (PSA):
Qualitative ranking of adsorption forces

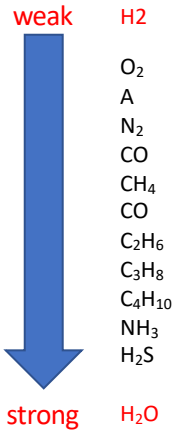

Natural Gas Steam Reforming

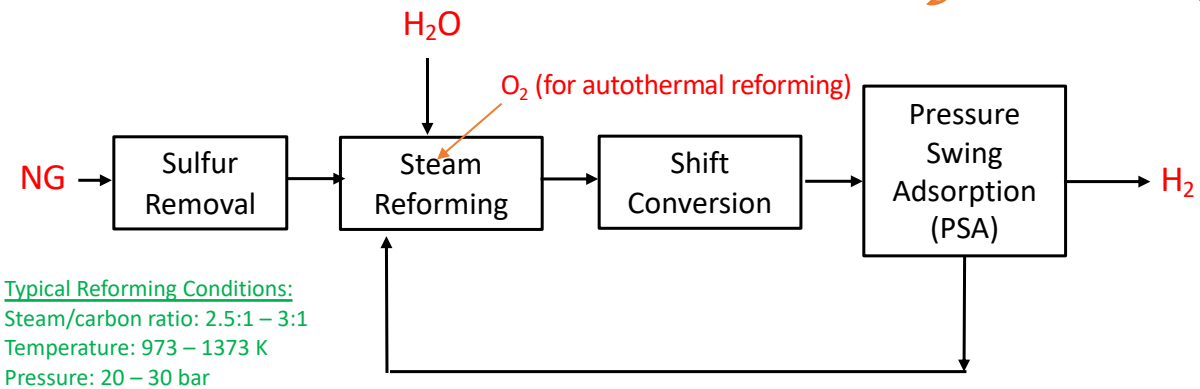

Typical Reforming Conditions:
Steam/carbon ratio: 2.5:1 – 3:1
Temperature: 973 – 1373 K
Pressure: 20 – 30 bar

Reforming reactions

$$C_nH_m + n\,H_2O \rightleftarrows n\,CO + \left(\frac{2n+m}{2}\right) H_2$$

$$CH_4 + H_2O \rightleftarrows CO + 3\,H_2$$

Water-Gas Shift reaction

$$CO + H_2O \rightleftarrows CO_2 + H_2$$

Natural Gas composition (wt-%)

Species	Formula	Mole-%
methane	CH4	93.037
ethane	C2H6	3.7
propane	C3H8	0.9
n-butane	nC4H10	0.13
i-butane	iC4H10	0.29
pentane	iC5H12	0.07
benzene	C6H6	0.07
sulfur dioxide	H2S	0.02
carbon dioxide	CO2	1.1
nitrogen	N2	0.68
oxygen	O2	0.001
helium	He	0.001
argon	Ar	0.001

Syngas composition:
Steam reforming at
1 atm, 1200 K

Species	kmol/s	mole fraction
CO	5.94E-02	2.51E-01
CO2	4.88E-04	2.06E-03
H2	1.73E-01	7.32E-01
H2O	1.96E-03	8.29E-03
H2S	1.15E-08	4.84E-08
SO2	1.19E-17	5.01E-17
HCl	1.00E-12	4.22E-12
Cl2	7.51E-33	3.17E-32
O2	4.77E-21	2.02E-20
N2	3.89E-04	1.64E-03
NH3	1.18E-06	4.98E-06
COS	1.24E-10	5.25E-10
CH4	1.19E-03	5.03E-03
He + Ar	1.15E-06	4.84E-06

Syngas composition:
Autothermal steam reforming
at 1 atm, 1200 K

Species	kmol/s	mole fraction
CO	4.233E-02	1.77E-01
CO2	1.875E-02	7.85E-02
H2	1.103E-01	4.61E-01
H2O	6.729E-02	2.82E-01
H2S	1.145E-08	4.79E-08
SO2	5.462E-14	2.29E-13
HCl	1.000E-12	4.18E-12
Cl2	1.181E-32	4.94E-32
O2	1.400E-17	5.86E-17
N2	3.893E-04	1.63E-03
NH3	5.924E-07	2.48E-06
COS	1.391E-10	5.82E-10
CH4	6.254E-06	2.62E-05
He + Ar	1.145E-06	4.79E-06

Biomass Gasification

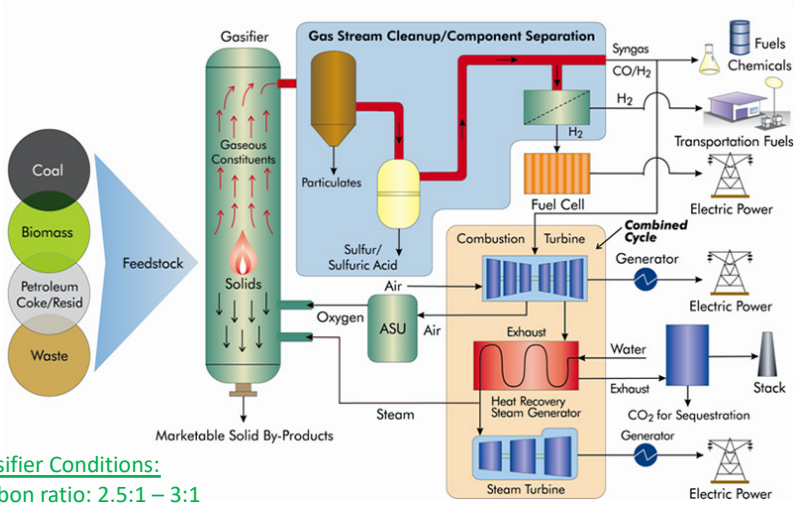

Typical Gasifier Conditions:
Steam/carbon ratio: 2.5:1 – 3:1
Temperature: 1073 – 1373 K
Pressure: 20 bar

Gasification reactions

$$C + H_2O \rightarrow CO + H_2$$
$$C + 2H_2O \rightarrow CO_2 + 2H_2$$
$$C + CO_2 \rightarrow 2CO$$

Water-gas shift reaction

$$CO + H_2O \rightarrow CO_2 + H_2$$

CO_2 in any exhaust stream is captured and stored.

Biomass composition

Corn Stover	
Proximate Analysis	wt-%
fixed carbon	20.0
volatile matter	68.9
moisture	~6.0
ash	5.1
Ultimate Analysis	wt-%
C	41.27
H	5.28
O	41.95
N	0.34
S	0.065

Autothermal steam gasification at 1 atm, 1200 K
Syngas composition

Species	moles/s	mole fraction
CO	1.655E+01	1.010E-01
CO2	1.782E+01	1.087E-01
H2	5.208E+01	3.179E-01
H2O	7.726E+01	4.715E-01
H2S	2.027E-02	1.237E-04
SO2	8.288E-07	5.059E-09
HCl	2.821E-13	1.722E-15
Cl2	1.989E-36	1.214E-38
O2	5.670E-14	3.461E-16
N2	1.213E-01	7.406E-04
NH3	1.566E-04	9.561E-07
COS	2.038E-04	1.244E-06
CH4	4.776E-04	2.915E-06

Biomass/Algae Fermentation

Microbial biomass conversion processes take advantage of the ability of microorganisms to consume and digest biomass and release hydrogen.

Dark fermentation is carried out by anaerobes in the absence of light and oxygen. In dark fermentation, bacteria act on the substrate and generate hydrogen.

The temperature range of dark fermentative hydrogen production is from 25 to 80°C, depending on the thermophilic degree of the bacteria.

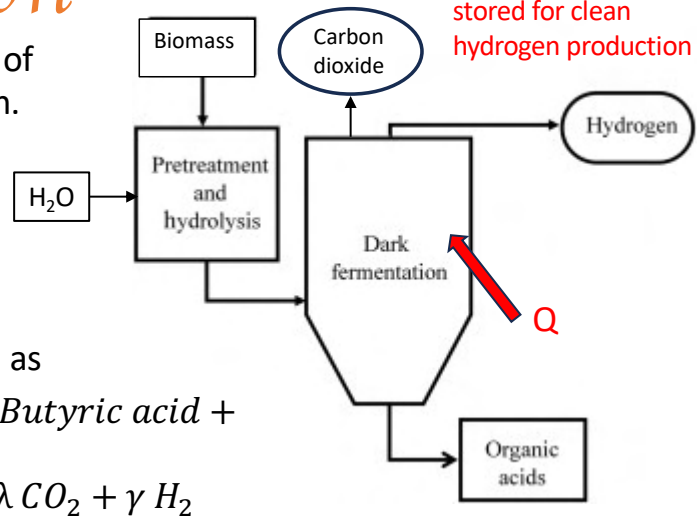

The general biochemical reaction in dark fermentation can be written as

$$a\ Biomass + b\ H_2O \longrightarrow \alpha\ Acetic\ acid + \beta\ Propionic\ acid + \delta\ Butyric\ acid + \varepsilon\ valeric\ acid + \theta\ hexanoic\ acid + \kappa\ Microbial\ biomass + ethanol + \lambda\ CO_2 + \gamma\ H_2$$

$$C_6H_{12}O_6 + H_2O \longrightarrow 2.5\ CH_3COOH + CO_2 + 2\ H_2$$

Various hydrogen-producing microbial strains and their H_2 yields (Zhang, et al., Biomass, Biofuels, Biochemicals, 2022, 141-159)

Strain	Substrate	Hydrogen yield
Rohobatersphaetoide RV	Wheat straw	1.23 mol H_2/mol glucose
Rohobatersphaetoide (NRLL B-1727)	Wheat straw	0.81 mol H_2/mol glucose
Rohobatersphaetoide (DSZM-158)	Wheat straw	0.97 mol H_2/mol glucose
Rhodobactercapsulatus JP91	Beet molasses	10.05 mol H_2/mol sucrose
Enterobacter aerogens	Molasses	0.52 mol H_2/mol substrate
Clostridium butyricum	Glucose	1.4–2.3 mol H_2/mol substrate
Enterobacter cloacae IIT BT 08	Glucose	2.3 mol H_2/mol substrate
Citrobacter sp. Y19	Glucose	2.49 mol H_2/mol substrate
Rhodopseudomonas palustris P4	Glucose	2.76 H_2/mol substrate

Strain	Substrate	Hydrogen yield
Clostridium acetobutyricum M121	Glucose	2.29 H_2/mol substrate
Clostridium tyrobutyricum FYa102	Glucose	1.47 H_2/mol substrate
Clostridium beijerinckii L9	Glucose	2.81 H_2/mol substrate
Clostridium thermocellum 27405	Delignified wood fiber	1.6 H_2/mol substrate
Mixed microflor	Wheat starch	1.9 H_2/mol substrate
Mixed microflor	0.75% soluble starch	2.14 H_2/mol substrate
Consortium	Corn stalk pith	2.61 mol H_2/mol glucose
Consortium	Corncob	228.94 mmol H_2/L culture

Current Hydrogen Production

U. S. H_2 Production
10 MMT per year
(Percent by Source)

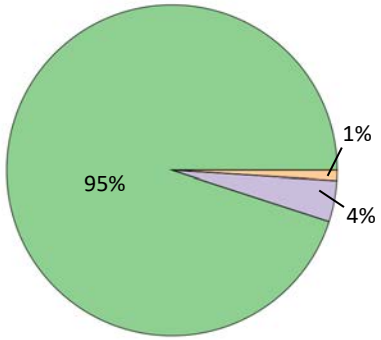

Global H_2 Production
70 MMT per year
(Percent by Source)

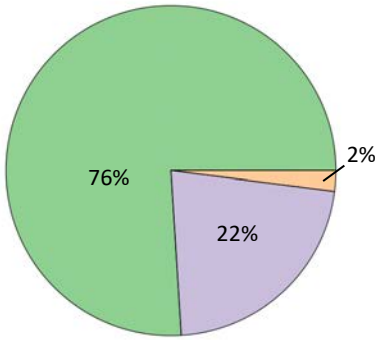

Reforming *Gasification* *Electrolysis*

Source: Hydrogen Strategy: Enabling A Low-Carbon Economy. Office of Fossil Energy, United States Department of Energy, Washington DC 20585

Potential Hydrogen Production Rates for
10 MW Energy Input to Process Unit

Method	Maximum H_2 Production (kg/day)	Transformation energy efficiency (%) [#]	Potential H_2 Production (kg/day)
PEM Water Electrolysis[+]	7,281[*]	50% - 70%	3,641 – 5,097
Methane Pyrolysis[++]	31,435[*]	58%	18,232
NG Autothermal Steam Reforming[**]	~ 400	75%	300
Corn Stover Gasification[***]	~ 280	35% - 50%	98 - 140

[*] Calculated from an exergy analysis; surroundings at 1 atm, 298 K
[+] Electrolysis at 350 K: electricity input = 10 MW; heat input from surroundings = 2.14 MW
[++] Pyrolysis at 1000 K: heat input at 1000 K = 10 MW; heat from surroundings = 1.65 MW
[**] Reforming at 1200 K, 1 atm; equilibrium syngas. Firing rate = $\dot{m}_{NG}(LHV)_{NG}$ = 10 MW
[***] Gasification at 1200 K, 1 atm; equilibrium syngas. Firing rate = $\dot{m}_{CS}(LHV)_{CS}$ = 10 MW
[#] Source: Ind. Eng. Chem. Res. 2021,60,32,11855-11881

Questions